Eur. Phys. J. C 5, 205–227 (1998)
DOI 10.1007/s100529800975

THE EUROPEAN PHYSICAL JOURNAL C

A measurement of the semileptonic branching ratio $\mathrm{BR}(\text{b-baryon} \to \mathrm{p}l\bar{\nu}X)$ and a study of inclusive $\pi^{\pm}$, $\mathrm{K}^{\pm}$, $(\mathrm{p}, \bar{\mathrm{p}})$ production in Z decays

The ALEPH Collaboration

R. Barate, D. Buskulic, D. Decamp, P. Ghez, C. Goy, J.-P. Lees, A. Lucotte, M.-N. Minard, J.-Y. Nief, B. Pietrzyk
Laboratoire de Physique des Particules (LAPP), IN^2P^3-CNRS, F-74019 Annecy-le-Vieux Cedex, France

G. Boix, M.P. Casado, M. Chmeissani, J.M. Crespo, M. Delfino, E. Fernandez, M. Fernandez-Bosman, Ll. Garrido[15], E. Graugès, A. Juste, M. Martinez, G. Merino, R. Miquel, Ll.M. Mir, I.C. Park, A. Pascual, J.A. Perlas, I. Riu, F. Sanchez
Institut de Física d'Altes Energies, Universitat Autònoma de Barcelona, E-08193 Bellaterra (Barcelona), Spain[7]

A. Colaleo, D. Creanza, M. de Palma, G. Gelao, G. Iaselli, G. Maggi, M. Maggi, N. Marinelli, S. Nuzzo, A. Ranieri, G. Raso, F. Ruggieri, G. Selvaggi, L. Silvestris, P. Tempesta, A. Tricomi[3], G. Zito
Dipartimento di Fisica, INFN Sezione di Bari, I-70126 Bari, Italy

X. Huang, J. Lin, Q. Ouyang, T. Wang, Y. Xie, R. Xu, S. Xue, J. Zhang, L. Zhang, W. Zhao
Institute of High-Energy Physics, Academia Sinica, Beijing, The People's Republic of China[8]

D. Abbaneo, R. Alemany, U. Becker, P. Bright-Thomas, D. Casper, M. Cattaneo, F. Cerutti, V. Ciulli, G. Dissertori, H. Drevermann, R.W. Forty, M. Frank, R. Hagelberg, J.B. Hansen, J. Harvey, P. Janot, B. Jost, I. Lehraus, P. Mato, A. Minten, L. Moneta, A. Pacheco, J.-F. Pusztaszeri[23], F. Ranjard, L. Rolandi, D. Rousseau, D. Schlatter, M. Schmitt, O. Schneider, W. Tejessy, F. Teubert, I.R. Tomalin, H. Wachsmuth, A. Wagner[20]
European Laboratory for Particle Physics (CERN), CH-1211 Geneva 23, Switzerland

Z. Ajaltouni, F. Badaud, G. Chazelle, O. Deschamps, A. Falvard, C. Ferdi, P. Gay, C. Guicheney, P. Henrard, J. Jousset, B. Michel, S. Monteil, J-C. Montret, D. Pallin, P. Perret, F. Podlyski, J. Proriol, P. Rosnet
Laboratoire de Physique Corpusculaire, Université Blaise Pascal, IN^2P^3-CNRS, Clermont-Ferrand, F-63177 Aubière, France

T. Fearnley, J.D. Hansen, J.R. Hansen, P.H. Hansen, B.S. Nilsson, B. Rensch, A. Wäänänen
Niels Bohr Institute, DK-2100 Copenhagen, Denmark[9]

G. Daskalakis, A. Kyriakis, C. Markou, E. Simopoulou, I. Siotis, A. Vayaki
Nuclear Research Center Demokritos (NRCD), GR-15310 Attiki, Greece

A. Blondel, G. Bonneaud, J.-C. Brient, P. Bourdon, A. Rougé, M. Rumpf, A. Valassi[6], M. Verderi, H. Videau
Laboratoire de Physique Nucléaire et des Hautes Energies, Ecole Polytechnique, IN^2P^3-CNRS, F-91128 Palaiseau Cedex, France

D.J. Candlin, M.I. Parsons
Department of Physics, University of Edinburgh, Edinburgh EH9 3JZ, United Kingdom[10]

T. Boccali, E. Focardi, G. Parrini, K. Zachariadou
Dipartimento di Fisica, Università di Firenze, INFN Sezione di Firenze, I-50125 Firenze, Italy

M. Corden, C. Georgiopoulos, D.E. Jaffe
Supercomputer Computations Research Institute, Florida State University, Tallahassee, FL 32306-4052, USA [13,14]

A. Antonelli, G. Bencivenni, G. Bologna[4], F. Bossi, P. Campana, G. Capon, V. Chiarella, G. Felici, P. Laurelli, G. Mannocchi[5], F. Murtas, G.P. Murtas, L. Passalacqua, M. Pepe-Altarelli
Laboratori Nazionali dell'INFN (LNF-INFN), I-00044 Frascati, Italy

L. Curtis, S.J. Dorris, A.W. Halley, J.G. Lynch, P. Negus, V. O'Shea, C. Raine, J.M. Scarr, K. Smith, P. Teixeira-Dias, A.S. Thompson, E. Thomson, F. Thomson
Department of Physics and Astronomy, University of Glasgow, Glasgow G12 8QQ,United Kingdom[10]

O. Buchmüller, S. Dhamotharan, C. Geweniger, G. Graefe, P. Hanke, G. Hansper, V. Hepp, E.E. Kluge, A. Putzer, J. Sommer, K. Tittel, S. Werner, M. Wunsch
Institut für Hochenergiephysik, Universität Heidelberg, D-69120 Heidelberg, Germany[16]

R. Beuselinck, D.M. Binnie, W. Cameron, P.J. Dornan, M. Girone, S. Goodsir, E.B. Martin, A. Moutoussi, J. Nash, J.K. Sedgbeer, P. Spagnolo, M.D. Williams
Department of Physics, Imperial College, London SW7 2BZ, United Kingdom[10]

V.M. Ghete, P. Girtler, E. Kneringer, D. Kuhn, G. Rudolph
Institut für Experimentalphysik, Universität Innsbruck, A-6020 Innsbruck, Austria[18]

A.P. Betteridge, C.K. Bowdery, P.G. Buck, P. Colrain, G. Crawford, A.J. Finch, F. Foster, G. Hughes, R.W.L. Jones, M.I. Williams
Department of Physics, University of Lancaster, Lancaster LA1 4YB, United Kingdom[10]

I. Giehl, A.M. Greene, C. Hoffmann, K. Jakobs, K. Kleinknecht, G. Quast, B. Renk, E. Rohne, H.-G. Sander, P. van Gemmeren, C. Zeitnitz
Institut für Physik, Universität Mainz, D-55099 Mainz, Germany[16]

J.J. Aubert, C. Benchouk, A. Bonissent, G. Bujosa, J. Carr, P. Coyle, C. Diaconu, F. Etienne, O. Leroy, F. Motsch, P. Payre, M. Talby, A. Sadouki, M. Thulasidas, K. Trabelsi
Centre de Physique des Particules, Faculté des Sciences de Luminy, IN^2P^3-CNRS, F-13288 Marseille, France

M. Aleppo, M. Antonelli, F. Ragusa
Dipartimento di Fisica, Università di Milano e INFN Sezione di Milano, I-20133 Milano, Italy

R. Berlich, W. Blum, V. Büscher, H. Dietl, G. Ganis, C. Gotzhein, H. Kroha, G. Lütjens, G. Lutz, C. Mannert, W. Männer, H.-G. Moser, R. Richter, A. Rosado-Schlosser, S. Schael, R. Settles, H. Seywerd, H. Stenzel, W. Wiedenmann, G. Wolf
Max-Planck-Institut für Physik, Werner-Heisenberg-Institut, D-80805 München, Germany[16]

J. Boucrot, O. Callot[2], S. Chen, Y. Choi[21], A. Cordier, M. Davier, L. Duflot, J.-F. Grivaz, Ph. Heusse, A. Höcker, A. Jacholkowska, D.W. Kim[12], F. Le Diberder, J. Lefrançois, A.-M. Lutz, I. Nikolic, M.-H. Schune, E. Tournefier, J.-J. Veillet, I. Videau, D. Zerwas
Laboratoire de l'Accélérateur Linéaire, Université de Paris-Sud, IN^2P^3-CNRS, F-91405 Orsay Cedex, France

P. Azzurri, G. Bagliesi[2], G. Batignani, S. Bettarini, C. Bozzi, G. Calderini, M. Carpinelli, M.A. Ciocci, R. Dell'Orso, R. Fantechi, I. Ferrante, L. Foà[1], F. Forti, A. Giassi, M.A. Giorgi, A. Gregorio, F. Ligabue, A. Lusiani, P.S. Marrocchesi, A. Messineo, F. Palla, G. Rizzo, G. Sanguinetti, A. Sciabà, J. Steinberger, R. Tenchini, G. Tonelli[19], C. Vannini, A. Venturi, P.G. Verdini
Dipartimento di Fisica dell'Università, INFN Sezione di Pisa, e Scuola Normale Superiore, I-56010 Pisa, Italy

G.A. Blair, L.M. Bryant, J.T. Chambers, M.G. Green, T. Medcalf, P. Perrodo, J.A. Strong, J.H. von Wimmersperg-Toeller
Department of Physics, Royal Holloway & Bedford New College, University of London, Surrey TW20 OEX, United Kingdom[10]

D.R. Botterill, R.W. Clifft, T.R. Edgecock, S. Haywood, P.R. Norton, J.C. Thompson, A.E. Wright
Particle Physics Dept., Rutherford Appleton Laboratory, Chilton, Didcot, Oxon OX11 OQX, United Kingdom[10]

B. Bloch-Devaux, P. Colas, S. Emery, W. Kozanecki, E. Lançon, M.-C. Lemaire, E. Locci, P. Perez, J. Rander, J.-F. Renardy, A. Roussarie, J.-P. Schuller, J. Schwindling, A. Trabelsi, B. Vallage
CEA, DAPNIA/Service de Physique des Particules, CE-Saclay, F-91191 Gif-sur-Yvette Cedex, France[17]

S.N. Black, J.H. Dann, R.P. Johnson, H.Y. Kim, N. Konstantinidis, A.M. Litke, M.A. McNeil, G. Taylor
Institute for Particle Physics, University of California at Santa Cruz, Santa Cruz, CA 95064, USA[22]

C.N. Booth, C.A.J. Brew, S. Cartwright, F. Combley, M.S. Kelly, M. Lehto, J. Reeve, L.F. Thompson
Department of Physics, University of Sheffield, Sheffield S3 7RH, United Kingdom[10]

K. Affholderbach, A. Böhrer, S. Brandt, G. Cowan, C. Grupen, P. Saraiva, L. Smolik, F. Stephan
Fachbereich Physik, Universität Siegen, D-57068 Siegen, Germany[16]

M. Apollonio, L. Bosisio, R. Della Marina, G. Giannini, B. Gobbo, G. Musolino
Dipartimento di Fisica, Università di Trieste e INFN Sezione di Trieste, I-34127 Trieste, Italy

J. Rothberg, S. Wasserbaech
Experimental Elementary Particle Physics, University of Washington, WA 98195 Seattle, USA

S.R. Armstrong, E. Charles, P. Elmer, D.P.S. Ferguson, Y. Gao, S. González, T.C. Greening, O.J. Hayes, H. Hu, S. Jin, P.A. McNamara III, J.M. Nachtman[24], J. Nielsen, W. Orejudos, Y.B. Pan, Y. Saadi, I.J. Scott, J. Walsh, Sau Lan Wu, X. Wu, J.M. Yamartino, G. Zobernig
Department of Physics, University of Wisconsin, Madison, WI 53706, USA[11]

Received 1 December 1997 / Published online: 4 August 1998

Abstract. Inclusive $\pi^{\pm}$, $K^{\pm}$ and $(p, \bar{p})$ production is investigated using data recorded by the ALEPH detector between 1992 and 1994. The momentum spectra and multiplicities are measured separately in $Z \to b\bar{b}$, $Z \to c\bar{c}$ and $Z \to u\bar{u}, d\bar{d}, s\bar{s}$ decays. The number of protons found in b-hadron decays is used to estimate the fraction of b-baryons in b events to be $(10.2 \pm 0.7 \pm 2.7)\%$ assuming BR(b-baryon$\to$ pX) $= (58 \pm 6)\%$. From an additional study of proton-lepton correlations in b events, the branching ratio BR(b-baryon $\to$ p$l\bar{\nu}X$) $= (4.63 \pm 0.72 \pm 0.98)\%$ is obtained. The ratio BR(b-baryon $\to$ p$l\bar{\nu}X$)/BR(b-baryon $\to$ pX) is found to be $0.080 \pm 0.012 \pm 0.014$.

1 Introduction

The long-standing discrepancy between theoretical predictions and measurements of the semileptonic branching ratio of heavy hadrons [1] has been solved by calculations including higher-order corrections [2]. However, the puzzle of the different lifetimes of b-mesons and b-baryons remains. The ratio of lifetimes $\tau_{\text{b-baryon}}/\tau_{\text{B}^0}$ is predicted to be no smaller than 0.9 [3] while present measurements yield a value of 0.73 ± 0.08 [4]. Under the assumption that the semileptonic widths of all b-hadrons are the same, this ratio can be probed independently by a measurement of the semileptonic branching ratio of b-baryons and mesons. Given the experimental measurements of lifetimes, a significantly smaller semileptonic branching ratio is expected for b-baryons than for b-mesons. This expectation is supported by an OPAL measurement, yielding (7.0±1.2±0.7)% for the ratio BR(b-baryon → $\Lambda l\bar{\nu}X$)/BR(b-baryon → ΛX) [5].

The measurement of the absolute branching ratio BR(b-baryon → p$l\bar{\nu}X$) is presented here[1]. Its evaluation requires the knowledge of the overall number of b-baryons and hence an estimate is made of the b-baryon fraction f_{Λ_b}, derived from proton production in b-hadron decays. The ratio $R_{\text{p}l}$ = BR(b-baryon → p$l\bar{\nu}X$)/BR(b-baryon → pX) is expected to be a good estimator for BR(b-baryon→ lX). The ratio $R_{\text{p}l}$ is compared with the overall semileptonic branching ratio BR(b → lX) which is known more precisely than the corresponding branching ratio of any specific b-hadron state.

For the evaluation of f_{Λ_b}, b events are selected with the help of a b-tag algorithm, and protons are statistically identified by their specific energy loss in the detector. The main difficulty is to distinguish protons produced in b-hadron decay from those from fragmentation. The method used here is based on the impact parameter of the tracks and their angle with respect to the thrust axis. The two variables are independent and display good separation power between leading and non-leading particles.

[1] Charge conjugated modes are always included if not stated otherwise

[1] Now at CERN, 1211 Geneva 23, Switzerland
[2] Also at CERN, 1211 Geneva 23, Switzerland
[3] Also at Dipartimento di Fisica, INFN, Sezione di Catania, Catania, Italy
[4] Also Istituto di Fisica Generale, Università di Torino, Torino, Italy
[5] Also Istituto di Cosmo-Geofisica del C.N.R., Torino, Italy
[6] Supported by the Commission of the European Communities, contract ERBCHBICT941234
[7] Supported by CICYT, Spain
[8] Supported by the National Science Foundation of China
[9] Supported by the Danish Natural Science Research Council
[10] Supported by the UK Particle Physics and Astronomy Research Council
[11] Supported by the US Department of Energy, grant DE-FG0295-ER40896
[12] Permanent address: Kangnung National University, Kangnung, Korea
[13] Supported by the US Department of Energy, contract DE-FG05-92ER40742
[14] Supported by the US Department of Energy, contract DE-FC05-85ER250000
[15] Permanent address: Universitat de Barcelona, 08208 Barcelona, Spain
[16] Supported by the Bundesministerium für Bildung, Wissenschaft, Forschung und Technologie, Germany
[17] Supported by the Direction des Sciences de la Matière, CEA
[18] Supported by Fonds zur Förderung der wissenschaftlichen Forschung, Austria
[19] Also at Istituto di Matematica e Fisica, Università di Sassari, Sassari, Italy
[20] Now at Schweizerischer Bankverein, Basel, Switzerland
[21] Permanent address: Sung Kyun Kwan University, Suwon, Korea
[22] Supported by the US Department of Energy, grant DE-FG03-92ER40689
[23] Now at School of Operations Research and Industrial Engineering, Cornell University, Ithaca, NY 14853-3801, USA
[24] Now at University of California at Los Angeles (UCLA), Los Angeles, CA 90024, USA

In parallel to the search for protons from b decays, charged particle production is studied in $Z \to b\bar{b}$, $Z \to c\bar{c}$ and $Z \to u\bar{u}, d\bar{d}, s\bar{s}$ events separately. The momentum spectra are measured for pions, kaons and protons and the corresponding mean multiplicities are calculated. These measurements are important to shed more light on the fragmentation of quarks and gluons into hadrons. At the same time, the measurement of the rates and momentum spectra of particles produced in b-hadron decays helps to assure a correct description of the weak decay of b-hadrons in the Monte Carlo simulation.

The following sections describe the detector and its performance, event and track selection, particle identification with dE/dx, the selection of b decay particles, proton-lepton correlations and the systematic uncertainties of the analysis. Conclusions summarizing the results are given at the end of the paper.

2 The detector

The ALEPH detector is described in detail elsewhere [6,7] and only a brief overview of the most relevant parts for this analysis is given here.

The momentum of charged particles is measured in three concentric tracking chambers. The innermost is the vertex detector consisting of two layers of double sided silicon microstrips with radii of 6.5 cm and 11.3 cm, respectively. The spatial resolution for the $r\phi$ and z projections is 12 μm at normal incidence. The vertex detector is surrounded by the inner drift chamber (ITC) with eight coaxial wire layers. Outside the ITC, the time projection chamber (TPC) provides up to 21 three-dimensional space points per track. The TPC has inner and outer radii of 30 and 180 cm and is 2.2 m long. The three tracking detectors are placed within a superconducting solenoid providing a magnetic field of 1.5 T, and together give a transverse momentum resolution of $\sigma(1/p_T) = 6 \times 10^{-4}(\mathrm{GeV}/c)^{-1}$ for high momentum tracks (p_T in GeV/c). The TPC also provides up to 338 measurements of the ionization loss of a track and is essential for the identification of charged particles. The specific energy loss dE/dx is estimated from the truncated mean of the usable samples associated with a track, discarding the lower 8% and upper 40% of the samples. For an electron with the full complement of measurements at a polar angle of $\Theta = 45°$, a resolution of 4.5% is achieved. About 88% of all tracks have at least 50 dE/dx samples. A more detailed description of the ALEPH dE/dx measurement can be found in [7] and [8].

The TPC is surrounded by a lead/proportional-chamber electromagnetic calorimeter segmented into $0.9° \times 0.9°$ projective towers and read out in three sections in depth with an energy resolution of $\sigma(E)/E = 0.18/\sqrt{E} + 0.009$ (E in GeV). In the electromagnetic calorimeter electrons and photons can be identified by their characteristic longitudinal and transverse shower developments. The iron return yoke of the magnet is instrumented with streamer tubes to form a hadron calorimeter and is surrounded by two additional double layers of streamer tubes to aid in muon identification.

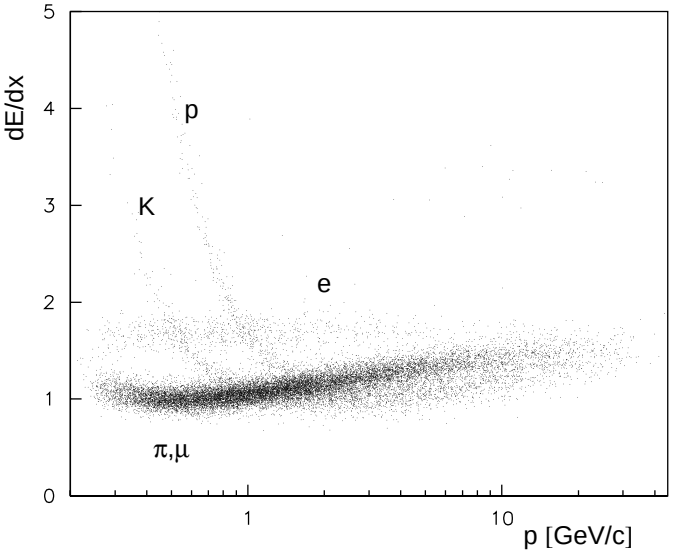

Fig. 1. The mean dE/dx of a sample of 20 000 tracks as a function of their momentum. The energy loss of minimal ionizing particles is normalized to one

The interaction point is reconstructed on an event-by-event basis using the constraint of the average beam spot position [7] resulting in an average resolution of 85 μm for $Z \to b\bar{b}$ events, projected along the sphericity axis of the event.

3 Event and track selection

The data used in this analysis were recorded by the ALEPH detector during the years 1992 – 1994. The selection of hadronic events is based on charged tracks and is described elsewhere [9]. Only events with a thrust axis fulfilling $|\cos\theta_{thrust}| < 0.85$ are taken into account leading to about 2.3 million selected hadronic Z decays with a residual contamination from $Z \to \tau\bar{\tau}$ determined from Monte Carlo to be 0.3%. Further cuts are applied on the quality of the tracks in these events. Each track must have at least four measured points in the TPC and at least 125 single dE/dx measurements. The tracks must originate from within a cylinder of radius 2 cm and length 20 cm centred on the nominal interaction point. The polar angle of the tracks must satisfy $|\cos\theta_{track}| < 0.85$ and a minimum momentum of 300 MeV/c is required. To avoid protons arising from interactions with the detector material, only negatively charged tracks are selected for momenta lower than 3 GeV/c.

4 Particle identification

Charged particles are identified by their specific energy loss in the TPC. Fig. 1 shows the truncated mean dE/dx as a function of the momentum for selected tracks from hadronic events. The number of pions, kaons and protons are obtained from the tracks' dE/dx distribution

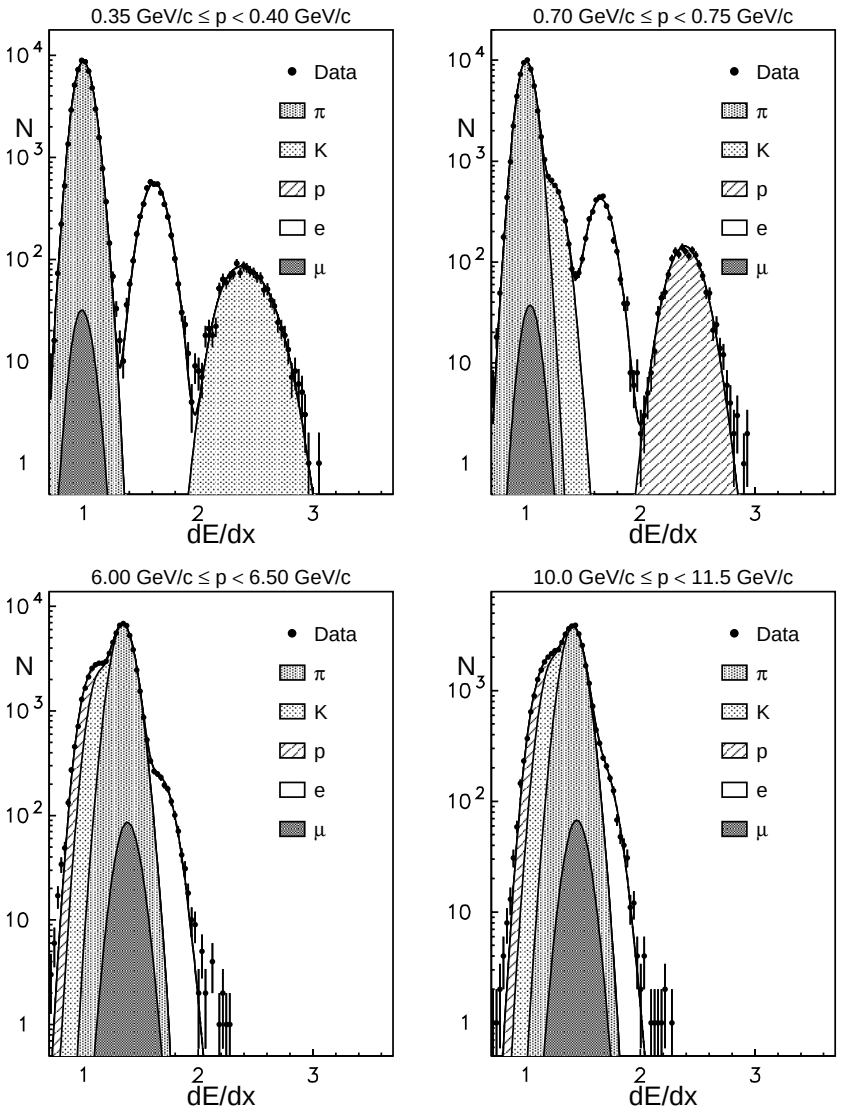

Fig. 2. Specific energy loss of selected particles together with the likelihood fit result in different momentum bins. The full dots represent the data, the hatched regions indicate the different particle fractions and the line is the overall fit function

by means of an extended maximum likelihood fit. The probability density, $G^j(\mathrm{d}E/\mathrm{d}x)$, for a given particle with a measured energy loss $\mathrm{d}E/\mathrm{d}x$ under the particle hypothesis $j = \pi, \mathrm{K}, \mathrm{p}, \mathrm{e}, \mu$ has been parametrized in a similar way to [8] but for this analysis a 'bifurcated' Gaussian has been used to allow a better description of the asymmetric tails of the $\mathrm{d}E/\mathrm{d}x$ distribution:

$$G^j(\mathrm{d}E/\mathrm{d}x) = \frac{2}{\sqrt{2\pi}(\sigma_+ + \sigma_-)} \times \exp\left(-\frac{(\mathrm{d}E/\mathrm{d}x - \langle \mathrm{d}E/\mathrm{d}x\rangle^j_{\mathrm{exp}})^2}{2\sigma^2_\pm}\right), \quad (1)$$

with $\sigma_\pm = \sigma_-$ for $\mathrm{d}E/\mathrm{d}x < \langle \mathrm{d}E/\mathrm{d}x\rangle^j_{\mathrm{exp}}$ and $\sigma_\pm = \sigma_+$ for $\mathrm{d}E/\mathrm{d}x \geq \langle \mathrm{d}E/\mathrm{d}x\rangle^j_{\mathrm{exp}}$, while $\langle \mathrm{d}E/\mathrm{d}x\rangle^j_{\mathrm{exp}}$ stands for the expected energy loss under the particle hypothesis j. The σ_+ and σ_- are parametrized as

$$\sigma_+/\langle \mathrm{d}E/\mathrm{d}x\rangle_{\mathrm{exp}} = A\sigma_-/\langle \mathrm{d}E/\mathrm{d}x\rangle_{\mathrm{exp}} = A\sigma_0 {n_s}^{p_1} l^{p_2} (\langle \mathrm{d}E/\mathrm{d}x\rangle_{\mathrm{exp}})^{p_3}, \quad (2)$$

with A being a free parameter in the likelihood fit (which in general is found to be close to one). Here, n_s is the number of single $\mathrm{d}E/\mathrm{d}x$ measurements, and l is the normalized mean sample length per measurement. The exponents p are expected to be close to 0.5 [10]. Together with σ_0 they were determined to be $p_1 = -0.5$, $p_2 = p_3 = -0.4$ and $\sigma_0 = 0.82$ from identified, low momentum particles [7]. The expected energy loss per unit length $\langle \mathrm{d}E/\mathrm{d}x\rangle^j_{\mathrm{exp}}$ is given by the Bethe-Bloch formula [11], a parametrization of which was fit to the ALEPH data from all particles in the low β region and from pions at higher momenta. Muons are not distinguished in the fit as their fraction is small with respect to the pions and hence it is fixed to the Monte Carlo prediction. The introduced uncertainties, mainly on the pion rates, are minor.

For the complete likelihood, the probability density is first summed over all possible particle types weighted with the corresponding particle fractions f_j (which are – together with A – the free parameters in the likelihood fit).

Then the probabilities of all tracks are multiplied:

$$\mathcal{L} = \frac{e^{-\phi}\phi^N}{N!} \prod_{i=1}^{N} \left(\sum_j f_j G_i^j \left(dE/dx^i, \langle dE/dx \rangle_{\exp}^{ji}, \sigma_{ji} \right) \right). \quad (3)$$

The Poisson factor in front represents the probability of obtaining a sample of size N from a distribution of mean ϕ, where ϕ is an additional free parameter in the fit. The sum of the particle fractions is constrained to one.

Some examples of the likelihood fit results are shown in Fig. 2 to illustrate the quality.

5 π, K and proton production

5.1 Decomposition of the track samples

All selected events are divided into two hemispheres, defined by the plane perpendicular to the thrust axis. On each hemisphere a b-tag is applied, based on the three-dimensional impact parameters of the tracks and giving the probability $\mathcal{P}_{uds}$ for this hemisphere to contain only tracks from the primary vertex. The performance of the b-tag is described in detail in [12]. Five intervals of the b-tag variable $\mathcal{P}_{uds}$ are defined and all tracks are assigned to one of these intervals according to the b-tag result of the opposite hemisphere in the same event. (The opposite hemisphere is used to minimize a possible bias introduced by the b-tag.) Using the tracks in each subsample, the likelihood fit gives the number of pions, kaons and protons for 50 different momentum bins. For each momentum bin, the composition of the particles regarding their primary quark flavour can be described for each of the five b-tag bins i by:

$$\begin{aligned} N_j^i &= \epsilon_{\rm b}^i N_j^{\rm b} + \epsilon_{\rm c}^i N_j^{\rm c} + \epsilon_{\rm uds}^i N_j^{\rm uds} \\ j &= \pi, {\rm K}, {\rm p};\ {\rm i} = 1 \ldots 5, \end{aligned} \quad (4)$$

where $N_j^{\rm b}$, $N_j^{\rm c}$ and $N_j^{\rm uds}$ are the (unknown) numbers of pions, kaons or protons in b, c, and uds hemispheres, and $\epsilon_{\rm b}^i$, $\epsilon_{\rm c}^i$ and $\epsilon_{\rm uds}^i$ are the fractions of b, c and uds hemispheres which fall in the b-tag interval i. Almost all the fractions ϵ^i can be derived from data following closely the method described in [12]. To do this, the number of hemispheres N^{H^i}, within a specific b-tag interval i, can be written as

$$N^{H^i} = (\epsilon_{\rm b}^i R_{\rm b} + \epsilon_{\rm c}^i R_{\rm c} + \epsilon_{\rm uds}^i R_{\rm uds}) N_{\rm tot}^H, \quad (5)$$

with $N_{\rm tot}^H$ being the total number of hemispheres, $R_{\rm b}$ the ratio of partial widths $\Gamma_{\rm Z\to b\bar{b}}/\Gamma_{\rm Z\to hadrons}$ and with $R_{\rm c}$ and $R_{\rm uds}$ being defined analogously to $R_{\rm b}$. The number of events N^{E^i} with both hemispheres in the same interval i is then given in terms of the total number of events selected, $N_{\rm tot}^E$, by

$$N^{E^i} = (\epsilon_{\rm b}^{D^i} R_{\rm b} + \epsilon_{\rm c}^{D^i} R_{\rm c} + \epsilon_{\rm uds}^{D^i} R_{\rm uds}) N_{\rm tot}^E, \quad (6)$$

with $\epsilon^{D^i} = \lambda^i {\epsilon^i}^2$ taking into account the correlation between the two hemispheres (of the order of 10%) by means of the factors λ^i. The λ^i values are taken from simulations. With the partial decay widths of the Z fixed to their Standard Model predictions (as given in [4]) and the constraint $\sum_i \epsilon_{\rm flav}^i = 1$ almost all fractions can be calculated from data. Only the three least significant fractions (out of fifteen) are fixed to their Monte Carlo predictions.

The number of pions, kaons and protons in $\mathrm{Z} \to \mathrm{b\bar{b}}$, $\mathrm{Z} \to \mathrm{c\bar{c}}$ and $\mathrm{Z} \to \mathrm{u\bar{u}}, \mathrm{d\bar{d}}, \mathrm{s\bar{s}}$ ($N_j^{\rm b}$, $N_j^{\rm c}$, $N_j^{\rm uds}$) is calculated from (4) for each momentum bin. The resulting momentum spectra are given in Fig. 7 to 9. They have been corrected for the effects of geometrical acceptance, track reconstruction efficiency and interactions in the material of the detector, using an event generator based on the DYMU [13] and JETSET 7.3 [14] programs, in which the decay properties of heavy flavour hadrons were significantly extended. The spectra are normalized to the number of hadronic Z decays and are the weighted mean of the three years of data taking. Background contamination of the hadronic event sample and efficiency of the selection cuts were determined by Monte Carlo simulation. The background from $\mathrm{Z} \to \tau\bar{\tau}$ decays was subtracted, the background from $\gamma\gamma \to$ hadrons is negligible. Gluon splittings into quark-/antiquark pairs are part of a hadronic events and therefore not suppressed by the selection of hadronic Z decays. The expectations of the Monte Carlo, which was tuned to reproduce global event shape and charged particle inclusive distributions [15], are indicated by the overlaid curves. The 'holes' in the spectra correspond to those momentum regions where the $\mathrm{d}E/\mathrm{d}x$ distributions of different particle types overlap so heavily that the fit is no longer sensitive to those particle fractions. These regions were excluded from the analysis. In the appendix the spectra are given in tabular form, a computer readable form can be found at [16].

To measure the number of particles coming directly from b-hadron decays, the track samples are further classified. Within each of the five b-tag intervals the tracks are divided into four classes: tracks with positive impact parameter, tracks with negative impact parameter, tracks with $|\cos\alpha| > 0.975$, where α is the angle between track and thrust axis, and tracks with $|\cos\alpha| < 0.975$. This leads to 20 different samples and hence, to 20 equations per particle type, describing the particle composition. In the following, the index j is omitted for simplicity:

$$\begin{aligned} N^{i,\rm class} = {} & \epsilon_{\rm b}^i \left(\epsilon_{\rm bdecay}^{\rm class} N_{\rm bdecay}^{\rm b} + \epsilon_{\rm accomp}^{\rm class} N_{\rm accomp}^{\rm b} \right) \\ & + \epsilon_{\rm c}^i \epsilon_{\rm c}^{\rm class} N^{\rm c} \\ & + \epsilon_{\rm uds}^i \epsilon_{\rm uds}^{\rm class} N^{\rm uds}, \end{aligned} \quad (7)$$

where $N^{i,\rm class}$ is the overall number of particles in the b-tag interval i fulfilling requirement 'class' (positive/negative impact parameter,$|\cos\alpha| < 0.975/ > 0.975$) and $N_{\rm bdecay}^{\rm b}$, $N_{\rm accomp}^{\rm b}$, $N^{\rm c}$ and $N^{\rm uds}$ are the number of particles from b decays, accompanying the b-hadron in b events, and the number in c events and uds events. The fraction of particles from b decays satisfying the criteria 'class' is indicated by $\epsilon_{\rm bdecay}^{\rm class}$, while $\epsilon_{\rm accomp}^{\rm class}$, $\epsilon_{\rm uds}^{\rm class}$ and $\epsilon_{\rm c}^{\rm class}$ are defined analogously. All these fractions are taken from Monte Carlo simulations. Then $N_{\rm bdecay}^{\rm b}$ and $N_{\rm accomp}^{\rm b}$ can

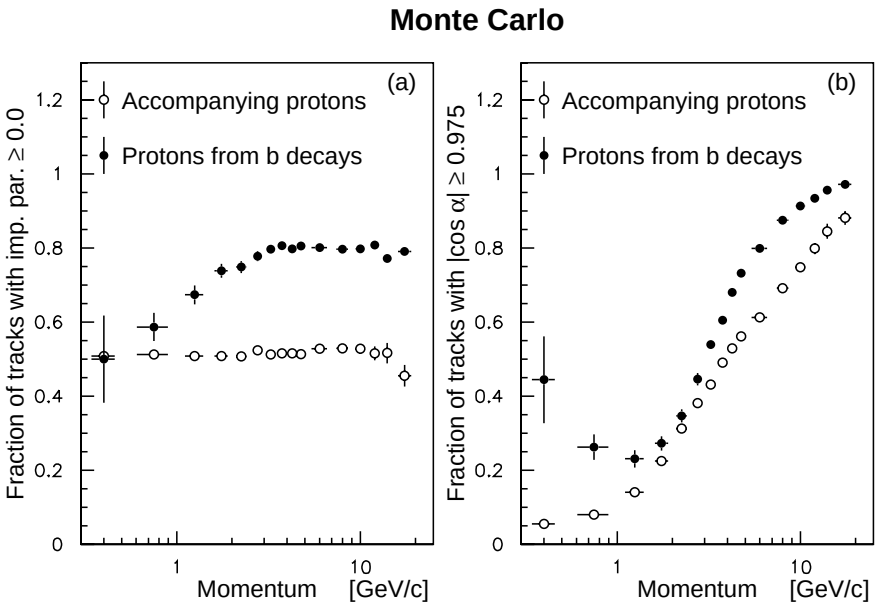

Fig. 3. a the fraction of protons with positive impact parameter depending on origin and momentum of the particle as predicted from Monte Carlo simulations of b-hadron decays. **b** the same for the fraction of protons with $|\cos\alpha| > 0.975$

be calculated from (4) and (7) if the difference between $\epsilon^{\rm class}_{\rm bdecay}$ and $\epsilon^{\rm class}_{\rm accomp}$ is sizeable. The separation power of the two variables is shown in Fig. 3, where in (a) the fractions of tracks with positive impact parameter are given for protons coming from b-hadron decays and for protons accompanying the b-hadron. It can be seen that particles from b-decays are more likely to have a positive impact parameter than accompanying particles due to the lifetime and the boost of the primary b-hadron. The discrimination on the basis of $|\cos\alpha| > 0.975$ is shown in Fig. 3 and takes advantage of the fact that decay products from b-hadron decays tend to be more collimated around the thrust axis (which is close to the flight direction of the b-hadron) than particles from the fragmentation.

After performing the likelihood fit for each sample, the numbers of pions, kaons and protons from b-hadron decays and accompanying the b-hadrons are calculated from (7) for all momentum bins. The resulting spectra are shown in Fig. 10 and 11. Below 1 GeV/c, the small number of protons from b decays is not accessible because of the high background from fragmentation protons.

5.2 Multiplicities

The momentum spectra of pions, kaons and protons in $Z \to b\bar{b}$, $Z \to c\bar{c}$, $Z \to u\bar{u}, d\bar{d}, s\bar{s}$ events, in b-hadron decays and accompanying the b-hadron in b events are shown in Figs. 7 to 11. After extrapolating the spectra over the full kinematic range with help of the simulated shapes, the corresponding mean multiplicities can be calculated. The overall normalization of the Monte Carlo was not used. The results are given in Tables 1 to 3.

A comparison with results from other e^+e^- experiments can be found in Tables 4, 5 and 6. In all cases, the agreement is very good. The proton production in b-hadron decays as measured at LEP is found to differ significantly from the Υ(4S) value. Adding the lepton multiplicity in b decays from Br(b → lX), Br(b → c → lX) [20] and Br(b → c$\bar{\rm c}$s → lX) [21] to the multiplicities of pions, kaons and protons in Table 6, the mean multiplicity

Table 1. Pion multiplicities in Z and b-hadron decays

origin	$\pi^\pm$				
$Z \to q\bar{q}$	17.04	$\pm$	$0.005_{\rm stat}$	$\pm$	$0.31_{\rm sys}$
$Z \to uds$	16.86	$\pm$	$0.02_{\rm stat}$	$\pm$	$0.52_{\rm sys}$
$Z \to c\bar{c}$	15.93	$\pm$	$0.07_{\rm stat}$	$\pm$	$1.31_{\rm sys}$
$Z \to b\bar{b}$	18.44	$\pm$	$0.03_{\rm stat}$	$\pm$	$0.63_{\rm sys}$
b decay	3.97	$\pm$	$0.02_{\rm stat}$	$\pm$	$0.21_{\rm sys}$

Table 2. Kaon multiplicities in Z and b-hadron decays

origin	$K^\pm$				
$Z \to q\bar{q}$	2.26	$\pm$	$0.002_{\rm stat}$	$\pm$	$0.12_{\rm sys}$
$Z \to uds$	2.14	$\pm$	$0.008_{\rm stat}$	$\pm$	$0.13_{\rm sys}$
$Z \to c\bar{c}$	2.44	$\pm$	$0.03_{\rm stat}$	$\pm$	$0.23_{\rm sys}$
$Z \to b\bar{b}$	2.63	$\pm$	$0.008_{\rm stat}$	$\pm$	$0.14_{\rm sys}$
b decay	0.72	$\pm$	$0.020_{\rm stat}$	$\pm$	$0.06_{\rm sys}$

Table 3. Proton multiplicities in Z and b-hadron decays

origin	$p, \bar{p}$				
$Z \to q\bar{q}$	1.00	$\pm$	$0.002_{\rm stat}$	$\pm$	$0.07_{\rm sys}$
$Z \to uds$	1.04	$\pm$	$0.006_{\rm stat}$	$\pm$	$0.07_{\rm sys}$
$Z \to c\bar{c}$	0.87	$\pm$	$0.02_{\rm stat}$	$\pm$	$0.10_{\rm sys}$
$Z \to b\bar{b}$	1.00	$\pm$	$0.007_{\rm stat}$	$\pm$	$0.08_{\rm sys}$
b decay	0.131	$\pm$	$0.004_{\rm stat}$	$\pm$	$0.011_{\rm sys}$

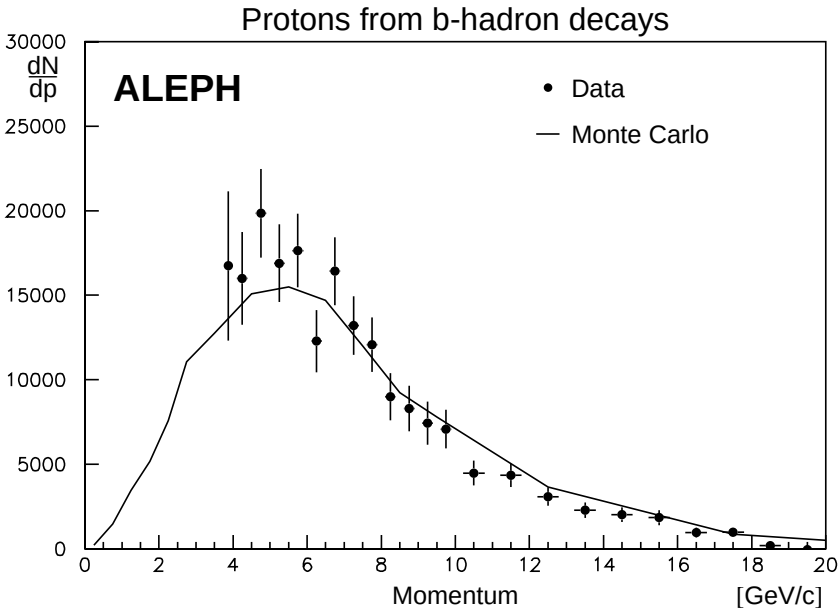

Fig. 4. Momentum spectrum for protons from b decays: data and Monte Carlo prediction. The Monte Carlo is normalized to the data

Table 4. Mean multiplicity of different particles in $Z \to q\bar{q}$ in comparison with DELPHI [17] and OPAL [18]

Mean multiplicities in Z → qq̄			
	this analysis	DELPHI	OPAL
$\pi^{\pm}$	17.04 ± 0.31	—	17.05 ± 0.43
$K^{\pm}$	2.26 ± 0.12	2.26 ± 0.18	2.42 ± 0.13
$p, \bar{p}$	1.00 ± 0.07	1.07 ± 0.14	0.92 ± 0.11

Table 5. Mean multiplicities of different particles in $Z \to b\bar{b}$ in comparison with DELPHI results [19]

Mean multiplicities in Z → bb̄		
	this analysis	DELPHI
$\pi^{\pm}$	18.44 ± 0.63	—
$K^{\pm}$	2.63 ± 0.14	2.74 ± 0.50
$p, \bar{p}$	1.00 ± 0.08	1.13 ± 0.27

Table 6. Mean multiplicities of pions, kaons and protons in b-hadron decays in comparison to DELPHI measurements [19] and to measurements by ARGUS and CLEO in Υ(4S) decays [4]. In contrast to Z decays only $B^{\pm}$ and B^0 are produced there, leading to a significant lower proton production from b decays

Mean multiplicities in b-hadron decays			
	this analysis	DELPHI	ARGUS/CLEO
$\pi^{\pm}$	3.97 ± 0.21	—	4.11 ± 0.08
$K^{\pm}$	0.72 ± 0.06	0.88 ± 0.19	0.78 ± 0.03
$p, \bar{p}$	0.131 ± 0.011	0.141 ± 0.059	0.08 ± 0.004

of charged particles in b decays is found to be

$$\langle n_{\mathrm{b}} \rangle = 5.24 \pm 0.25 \ . \tag{8}$$

The result is dominated by systematics and can be compared with measurements of DELPHI [19] and OPAL [22] which gave $\langle n_{\mathrm{b}} \rangle = 5.84 \pm 0.38$ and 5.51 ± 0.51, respectively.

5.3 The b-baryon fraction $f_{\Lambda_{\mathrm{b}}}$

The overall number of protons from b-hadron decay is used to estimate $f_{\Lambda_{\mathrm{b}}}$, the fraction of b-baryons found in b events near the Z resonance. Assuming that BR(b-baryon → pX) is considerably larger than BR(b-meson → pX), even a small fraction of b-baryons will lead to a sizeable increase of protons in b-hadron decays with respect to the pure meson sample, as in Υ(4S) decays.

The number of protons from b-hadron decays N_{p} is related to the b-baryon fraction as follows

$$\begin{aligned} N_{\mathrm{p}} = (& f_{\Lambda_{\mathrm{b}}} \mathrm{BR(b\text{-}baryon} \to \mathrm{p}X) \\ & + (1 - f_{\Lambda_{\mathrm{b}}}) \mathrm{BR(b\text{-}meson} \to \mathrm{p}X)) N_{\mathrm{b}} \end{aligned} \tag{9}$$

with the number of b-hadron decays N_{b} being calculated from the overall number of events multiplied by $2R_{\mathrm{b}}$ (using the Standard Model value for R_{b}). The equation can be solved for $f_{\Lambda_{\mathrm{b}}}$:

$$f_{\Lambda_{\mathrm{b}}} = \frac{N_{\mathrm{p}}/N_{\mathrm{b}} - \mathrm{BR(b\text{-}meson} \to \mathrm{p}X)}{\mathrm{BR(b\text{-}baryon} \to \mathrm{p}X) - \mathrm{BR(b\text{-}meson} \to \mathrm{p}X)} \ . \tag{10}$$

To extract N_{p}, the measured momentum spectra of b decay protons is extrapolated from 3.75 GeV/c to zero using the Monte Carlo prediction as indicated in Fig. 4. The ratio $N_{\mathrm{p}}/N_{\mathrm{b}}$ is the mean proton multiplicity in b-hadron decays as given in Table 6. The branching ratio

$BR(B^{\pm}, B^0 \to pX)$ has been measured at the $\Upsilon(4S)$ by ARGUS and CLEO to be $(8.0 \pm 0.4)\%$ [4] but $BR(B_s \to pX)$ is unknown. As a conservative estimate $BR(B_s \to pX) = (8.0 \pm 4.0)\%$ has been assumed. For the calculation of the error, a B_s fraction in b events of $(11.2 \pm 1.9)\%$ was taken from [4].

Since no measurement exists for BR(b-baryon → pX), it has to be estimated. Naively BR(b-baryon → pX) is close to BR(b-baryon → nX) and hence about 50%. But this assumption does not fully hold true, taking e.g. isospin arguments and the decay via Λ or Σ particles into account, which lead to different branching ratios into protons and neutrons. As an upper limit one can assume that all b-baryon decays produce a Λ and therefore BR(b-baryon → pX) = 64%. For a lower estimate BR(b-baryon → ΛX) = BR(b-baryon → $\Sigma^+ X$) = BR(b-baryon → $\Sigma^0 X$) = BR(b-baryon → $\Sigma^- X$) = 25% has been assumed. This results in BR(b-baryon → pX) = 45%. The mean value is $(54.5 \pm 5.5)\%$. The error is taken from the standard deviation of a uniform probability distribution. The range is large enough to accommodate contributions from direct b-baryon and c-baryon decays to protons. However, according to the Monte Carlo, 3% of all b-baryon decays involve decays into three baryons in the final state. This contributes an additional $(3.3 \pm 1.6)\%$ to the above estimate. Hence BR(b-baryon → pX) = $(58 \pm 6)\%$ has been used for the calculation of the b-baryon fraction. The result is

$$f_{\Lambda_b} = (10.2 \pm 0.7_{\rm stat} \pm 2.2_{\rm sys1} \pm 1.6_{\rm sys2})\%. \qquad (11)$$

Here the first systematic error includes uncertainties related to the analysis and the second includes the uncertainties related to the branching ratios. The systematic uncertainties of the measurement are discussed in Sect. 7. The resulting baryon fraction can be compared to the value (13.2±4.1)% calculated from BR(b-baryon → $\Lambda_c l\bar{\nu}X$) and the b-baryon lifetime [4] and is found to be in good agreement.

6 Proton-lepton correlation

For the search for proton-lepton[2] pairs from b-baryon decays, the analysis is restricted to events containing a high momentum lepton candidate. The selection of leptons within ALEPH is discussed in [20] and [23]. Electrons and muons are required to have momenta greater then 2 GeV/c and 3 GeV/c, respectively. For this analysis, only tracks with opposite charge with respect to the lepton candidate are selected. The angle between the track and the thrust axis is not used because of possible correlations with the transverse momentum of the lepton. The selection cuts for the tracks, as described in Sect. 3, are slightly released to gain efficiency but a minimum momentum of 4 GeV/c is required. No b-tag is performed. The presence of a high momentum lepton candidate enriches the event sample with b events by almost a factor of three relative to the nominal b content corresponding to R_b.

[2] 'lepton' stands for electron or muon

Table 7. Composition of the proton-lepton sample with protons coming from b-hadron decays. The Monte Carlo predictions for b-baryon → $pl\bar{\nu}X$ and $b \to \tau\bar{\nu}pX$, $\tau \to l\bar{\nu}\nu$ have been reweighted to reflect the lifetime difference between b-baryons and b-mesons. As indicated, two contributions are fixed within the fit. No meaningful distinction between the different background sources could be achieved. Therefore only the overall number is given here

Composition of the proton-lepton pair sample		
Source	MC prediction	fit result
b-baryon decays	3071	2987 ± 418
$b \to c\bar{c}s, \bar{c} \to l\bar{\nu}X$	667 (fixed)	
$b \to \tau\bar{\nu}pX$, $\tau \to l\bar{\nu}\nu$	133 (fixed)	
b-meson → $\Lambda_c\bar{p}X$, $\Lambda_c \to l\bar{\nu}X$	2247	
b-meson → $\bar{p}l\bar{\nu}X$	222	
b → pX+ fake lepton	1407	
Total background	4676	4686 ± 643
Sum	7747	7673 ± 613

The number of proton-lepton pairs are evaluated from the dE/dx distribution of the tracks. The impact parameter of the protons are again used to measure their number in b decays while the p_T of the lepton with respect to the jet axis (calculated without the lepton) is used to identify the proton-lepton pairs from b-baryons and separate them from background processes. Possible background sources for proton-lepton pairs are listed below:

1. Decay of the b quark into c$\bar{c}$s with subsequent semileptonic $\bar{c}$ quark decay in $l^- X$. An example is the decay $\Lambda_b \to \bar{D}_s pX$, $\bar{D}_s \to l^- X$. Using BR(b → c$\bar{c}$s, $\bar{c} \to lX$) = $(1.3 \pm 0.5)\%$ [21] and BR(b-baryon → pX) = $(58 \pm 6)\%$ about 0.8% of all b-baryons are expected to contribute to this background. A similar assumption can be made for mesons. With BR(b-meson → pX) = 8% [4], approximately 0.04% of all b-mesons and therefore 0.12% of all b-hadrons are expected to contribute to this background.
2. b-baryon → pτX with subsequent leptonic decay of the τ lepton. From the known branching ratio of b → τX one can conclude that about 0.02% of all b-hadrons contribute to this background source.
3. b-meson → $\Lambda_c\bar{p}X$ followed by a semileptonic decay of the Λ_c.
4. b-meson → $\bar{p}lX$.
5. The lepton is produced in pion or kaon decays, in photon conversion or is a misidentified hadron. In the following these will be called 'fake leptons'.

All background processes (summarized in Table 7) have considerably softer lepton p_T spectra than the signal process.

In total 14 385 proton-lepton pairs are identified. They are divided in eight different sets. Four intervals, based on the p_T of the lepton candidate, 0.0 and 0.5 GeV/c, 0.5 and

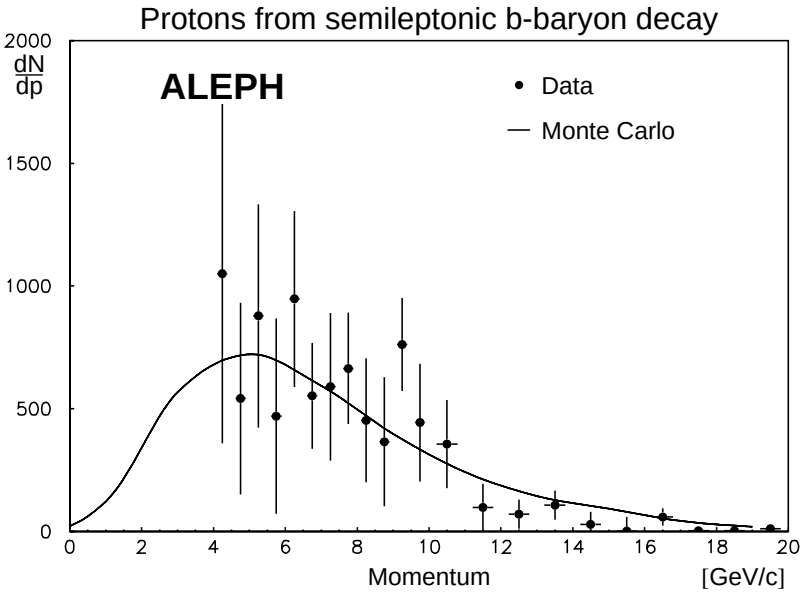

Fig. 5. The momentum spectrum of protons from semileptonic b-baryon decay (electrons and muons). The dots represent the data, the line the Monte Carlo prediction, normalized to the data

0.8 GeV/c, 0.8 and 1.2 GeV/c and greater than 1.2 GeV/c are chosen and then each set is divided further into one sample containing tracks with positive impact parameters and one containing tracks with negative impact parameters. The number of protons in each sample can be written as:

$$N^{\mathrm{p}l}_{\hat{p_T},+} = \epsilon^{+}_{\mathrm{b}} \left(\sum_x \epsilon^{x}_{\hat{p_T}} N^{x}_{\mathrm{p}l} \right) + \epsilon^{+}_{\text{non-b}} N^{\text{non-b}}_{\hat{p_T}}$$
$$N^{\mathrm{p}l}_{\hat{p_T},-} = \epsilon^{-}_{\mathrm{b}} \left(\sum_x \epsilon^{x}_{\hat{p_T}} N^{x}_{\mathrm{p}l} \right) + \epsilon^{-}_{\text{non-b}} N^{\text{non-b}}_{\hat{p_T}}, \quad (12)$$

with $N^{\mathrm{p}l}_{\hat{p_T},+}$ being the measured number of proton-lepton pairs with a transverse momentum of the lepton candidate in the p_T interval $\hat{p_T}$ and a proton with positive impact parameter, $N^{\mathrm{p}l}_{\hat{p_T},-}$ is defined analogously but contains protons with negative impact parameters. The numbers of proton-lepton pairs from the different sources x (b-baryon decay or one of the background processes described above) are denoted $N^{x}_{\mathrm{p}l}$ and are calculated together with the numbers of proton-lepton pairs $N^{\text{non-b}}_{\hat{p_T}}$ where the proton does not come from any b decay but the lepton candidate has a p_T in the interval $\hat{p_T}$. The fraction of leptons from source x having a transverse momentum in the p_T interval $\hat{p_T}$ is written as $\epsilon^{x}_{\hat{p_T}}$. The fraction of protons from b-hadron decays having a positive impact parameter is denoted $\epsilon^{+}_{\mathrm{b}}$ with $\epsilon^{+}_{\text{non-b}}$, $\epsilon^{-}_{\mathrm{b}}$ and $\epsilon^{+}_{\text{non-b}}$ defined analogously. All fractions are taken from the simulation. To solve the equations, two background contributions are fixed to the expected values as given in Table 7. The number of protons from b-baryon decays can then be calculated from the number of proton-lepton pairs in the four p_T intervals for each of the 22 momentum bins in Fig. 5. Overall 7673 proton-lepton pairs are found to contain a proton from b-hadron decay and 2987 are assigned to b-baryon decays. The sum of proton-lepton pairs from the background processes discussed above are in good agreement with the Monte Carlo expectation. However, the p_T distributions for the various background sources are so similar that it is not possible within this analysis to measure the individual fractions. The efficiency corrected proton spectrum for semileptonic b-baryon decays is given in Fig. 5. Extrapolating the spectrum to zero using Monte Carlo leads to

$$f_{\Lambda_{\mathrm{b}}} \mathrm{BR}(\text{b-baryon} \to \mathrm{p}l\bar{\nu}X) = (4.72 \pm 0.66_{\mathrm{stat}} \pm 0.44_{\mathrm{sys}})10^{-3} \; . \quad (13)$$

This number is the average of $l = electron$ and $l = muon$ and can be compared with a measurement of DELPHI [24]: $f_{\Lambda_{\mathrm{b}}}\mathrm{BR}(\text{b-baryon} \to \mathrm{p}\mu X) = (4.9 \pm 1.1 \pm 1.3)10^{-3}$. An absolute branching ratio can be calculated using $f_{\Lambda_{\mathrm{b}}}$ from (11):

$$\mathrm{BR}(\text{b-baryon} \to \mathrm{p}l\bar{\nu}X) = (4.63 \pm 0.72_{\mathrm{stat}} \pm 0.68_{\mathrm{sys1}} \pm 0.71_{\mathrm{sys2}})\% \; . \quad (14)$$

The systematic error has been split in two parts. While the first covers the systematic uncertainties related to the analysis, the second takes account of the uncertainties of branching ratio entering the calculation of $f_{\Lambda_{\mathrm{b}}}$. One of the major uncertainties is the estimate of BR(b-baryon → pX). However, the ratio $R_{\mathrm{p}l}$ = BR(b-baryon → p$l\bar{\nu}X$)/ BR(b-baryon → pX) is only slightly dependent on this quantity as indicated in Fig. 6. $R_{\mathrm{p}l}$ is found to be

$$R_{\mathrm{p}l} = \frac{(4.72 \pm 0.66_{\mathrm{stat}} \pm 0.44_{\mathrm{sys}})10^{-3}}{f_{\Lambda_{\mathrm{b}}}\mathrm{BR}(\text{b-baryon} \to \mathrm{p}X)} \; . \quad (15)$$

Inserting (10) leads to:

$$R_{\mathrm{p}l} = \frac{4.72 \cdot 10^{-3} \left(1 - \frac{\mathrm{BR(b\text{-}meson}\to \mathrm{p}X)}{\mathrm{BR(b\text{-}baryon}\to \mathrm{p}X)}\right)}{N_{\mathrm{p}}/N_{\mathrm{b}} - \mathrm{BR}(\text{b-meson} \to \mathrm{p}X)} = 0.080 \pm 0.012_{\mathrm{stat}} \pm 0.014_{\mathrm{sys}} \; . \quad (16)$$

Assuming that

$$\frac{\mathrm{BR(b\text{-}baryon} \to \mathrm{p}l\bar{\nu}X)}{\mathrm{BR(b\text{-}baryon} \to lX)} \approx \mathrm{BR(b\text{-}baryon} \to \mathrm{p}X) \quad (17)$$

the ratio $R_{\mathrm{p}l}$ is close to BR(b-baryon $\to lX$) and can be compared with the recent OPAL measurement [5] of $R_{\Lambda l} = 0.070 \pm 0.012 \pm 0.007$, with $R_{\Lambda l} = \mathrm{BR(b\text{-}baryon} \to \Lambda l\bar{\nu}X)/\mathrm{BR(b\text{-}baryon} \to \Lambda X)$, which is in very good agreement.

If

$$\frac{\tau_{\text{b-baryon}}}{\tau_{\mathrm{b}}} \approx \frac{\mathrm{BR(b\text{-}baryon} \to lX)}{\mathrm{BR(b} \to lX)} \quad (18)$$

and $R_{\mathrm{p}l} \approx \mathrm{BR(b\text{-}baryon} \to lX)$ one can compare the ratio of the semileptonic branching ratios of b-baryons and all b-hadrons

$$\frac{R_{\mathrm{p}l}}{\mathrm{BR(b} \to lX)} = 0.72 \pm 0.17 \quad (19)$$

with the corresponding ratio of lifetimes, calculated from [4]:

$$\frac{\tau_{\text{b-baryon}}}{\tau_{\mathrm{b}}} = 0.74 \pm 0.05\ . \quad (20)$$

The agreement is again very good. The branching ratio BR(b $\to lX$) in Z decays has been taken from [4].

7 Systematics

Several sources of systematic uncertainties affect the accuracies of the measurements. They are listed for f_{Λ_b} and BR(b-baryon → p$l\bar{\nu}X$) in Table 8 and 9 together with the uncertainties due to the limited knowledge of the branching ratios BR(b-baryon → pX) and BR(b-meson → pX).

The fitted particle rates depend crucially on the expected dE/dx values and resolutions entering the likelihood function. Therefore the expected dE/dx are shifted within the uncertainties of the parametrization of the Bethe-Bloch formula (Sect. 4). The resolution is rescaled and a Gaussian is used instead of a 'bifurcated' Gaussian. In the overlap region, the added uncertainties are 0.9%, 4% and 6.5% for pions, kaons and protons, respectively. The deviations of subsequent bins are correlated and conservatively all momentum bins within the overlap region are taken to be 100 % correlated while the rates of different particles are highly anti-correlated. No noticable bias due to the fit procedure was found.

The sign of a track's impact parameter and its angle with the thrust axis are used to distinguish particles from b-hadron decay from accompanying particles. Hence the result relies on the correct simulation of these two quantities. Two checks are performed: First no distinction is made between decay and fragmentation particles. Equation system (7) then reduces to:

$$\begin{aligned} N^i &= \epsilon^i_{\mathrm{b}} N_{\mathrm{b}} + \epsilon^i_{\mathrm{c}} N_{\mathrm{c}} + \epsilon^i_{\mathrm{uds}} N_{\mathrm{uds}} \\ N^{i,\mathrm{class}} &= \epsilon^{\mathrm{class}}_{\mathrm{b}} \epsilon^i_{\mathrm{b}} N_{\mathrm{b}} + \epsilon^{\mathrm{class}}_{\mathrm{c}} \epsilon^i_{\mathrm{c}} N_{\mathrm{c}} + \epsilon^{\mathrm{class}}_{\mathrm{uds}} \epsilon^i_{\mathrm{uds}} N_{\mathrm{uds}}\ . \end{aligned} \quad (21)$$

Again i indicates the five b-tag bins, N^i stands for the total number of particles (pions, kaons or protons) found in the bin i and $N^{i,\mathrm{class}}$ is the total number of particles in bin i fulfilling requirement 'class'. From the ten equations per 'class', the fractions $\epsilon^{\mathrm{class}}$ for particles in uds, c and b events can be derived directly from the data, and then be compared with the Monte Carlo predictions. At very low (high) momentum, $\epsilon^{\mathrm{class}}$ is very close to $\epsilon^{\mathrm{class}}_{\mathrm{accomp}}$ ($\epsilon^{\mathrm{class}}_{\mathrm{bdecay}}$).

Table 8. The different contributions to the two systematic errors on f_{Λ_b}. The quoted errors are absolute

Composition of the systematic errors on f_{Λ_b}	
1. Systematic uncertainties from the analysis	
dE/dx	1.7%
b-tag	0.8%
Imp. par. and $cos\alpha$	0.8%
Extrapolation	0.6%
Reconstr. efficiency	0.5%
Total	2.2%
2. Systematic uncertainties from branching ratios	
BR(b-meson → pX)	1.0%
BR(b-baryon → pX)	1.2%
Total	1.6%

For the second check, the number of particles from b-hadron decays is calculated from the positive impact parameter alone and the result is used to calculate the fraction fulfilling $|\cos\alpha| < 0.975$. In both cases the agreement between data and simulation is good and the maximal deviation is taken as the systematic uncertainty. All momentum bins are taken to be 100% correlated.

Attention is given to the numbers of protons coming from long-lived hyperons such as Λ or Σ. The fraction of protons coming from Λ decays in b decays has been changed by about 30% in the Monte Carlo to be in agreement with measurements of DELPHI [17] and OPAL [5]. The resulting change in the number of particles from b decays is found to be well covered by the systematic uncertainty of 3.5% derived from the two checks described above.

The fraction of tracks from b decays having a positive impact parameter depends on the lifetime of the parent b-hadron. Since one of the motivations of this measurement was to test the difference in lifetimes between b-baryons and b-mesons, the differences found in the impact parameter distribution between Monte Carlo samples with different b lifetimes are taken into account in the systematic uncertainties but are found to be negligible.

Several other sources of systematic uncertainties are investigated. The b-tag efficiencies lead to errors of 2.5%, 8%, 3% on the particle rates from uds-, c- and b-events, respectively, with a strong anti-correlation especially between uds and c events and between b and c events. The bias induced by the b-tag itself was found to be negligible. The mean uncertainty on the reconstruction efficiencies amounts to 1.5% and is common to all particle rates. The muon fraction in the likelihood fit and the efficiency correction for particles from nuclear interactions were varied

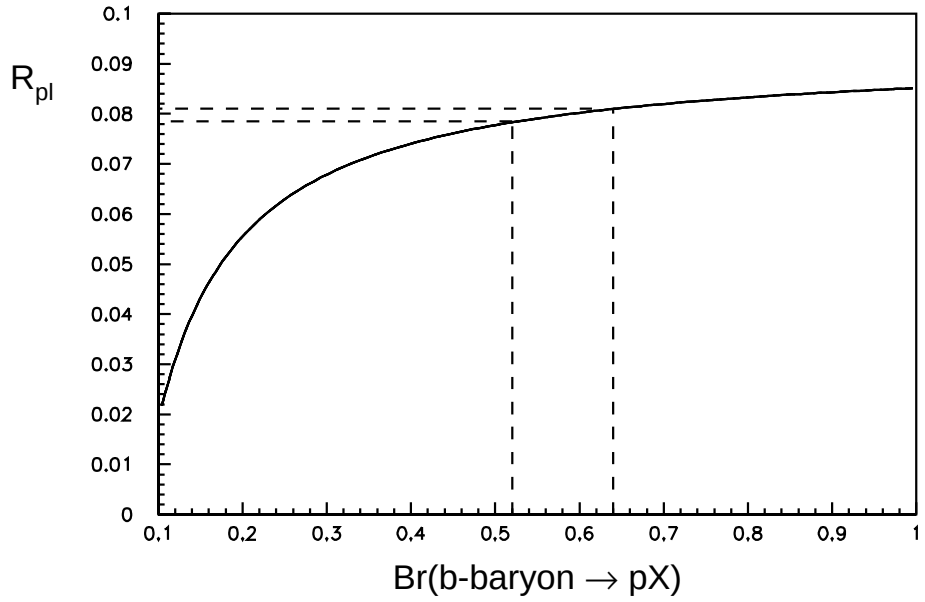

Fig. 6. The dependence of R_{pl} on BR(b-baryon $\rightarrow pX$). R_{pl} varies only slightly with BR(b-baryon $\rightarrow pX$) over a wide range. Allowing BR(b-baryon $\rightarrow pX$) to vary between 0.52 and 0.64, R_{pl} changes only by 0.003. Towards smaller BR(b-baryon $\rightarrow pX$) the dependence increases significantly

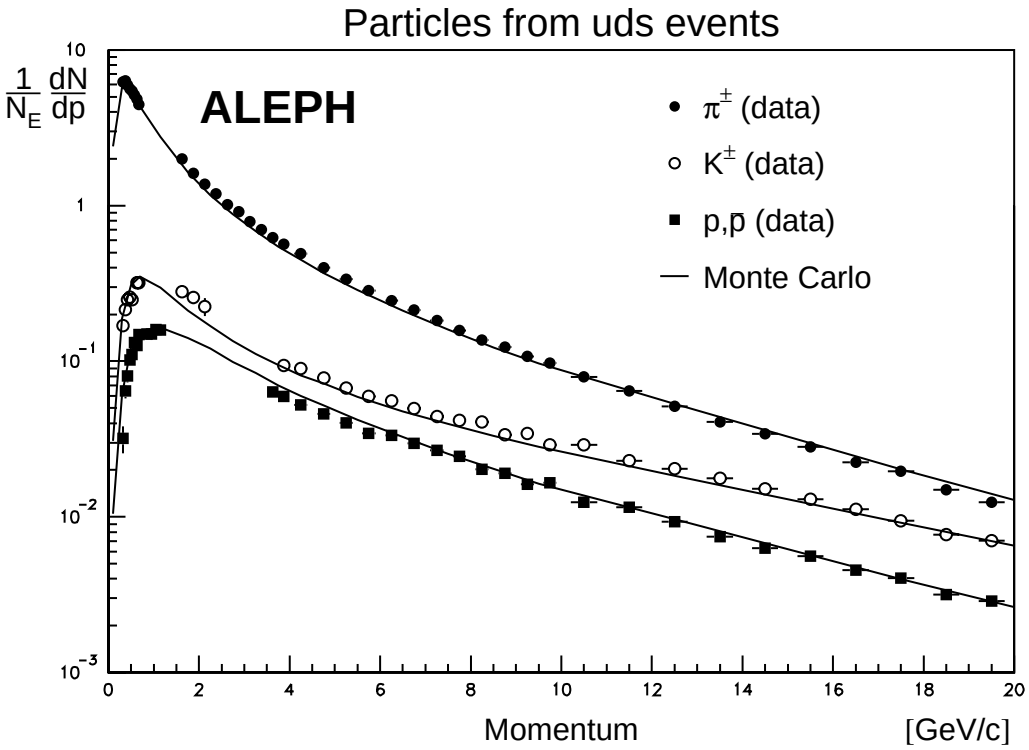

Fig. 7. Momentum spectra from pions, kaons and protons in uds events together with the Monte Carlo predictions. The errors shown are the quadratic sum of statistical and systematic errors

by 10% with respect to the Monte Carlo prediction. The effects are of no importance for protons from b-hadron decays but were included into the error calculation for the other multiplicities in Sect. 5.2.

The extrapolation of the measured momentum spectra over the whole momentum range has been checked by using HERWIG 5.6, JETSET 7.3 and JETSET 7.4 for the extrapolation and the JETSET prediction has been compared to the momentum spectra of protons from $B^{\pm}, B^0$ decays as measured by ARGUS [25] and CLEO [26] and found to be in good agreement.

Most of the uncertainties discussed above are also present in the proton-lepton analysis and partly cancel in the ratio f_{Λ_b}BR(b-baryon $\rightarrow$ p$l\bar{\nu}X$)$/f_{\Lambda_b}$. Additional uncertainties are due to lepton identification and the simulation of the lepton p_T spectra [20,23]. The impact of the fixed branching ratios (b $\rightarrow$ c$\bar{\text{c}}$s with semileptonic $\bar{\text{c}}$ decay and b-baryon $\rightarrow \tau\bar{\nu}pX$) is small and variations of 50%

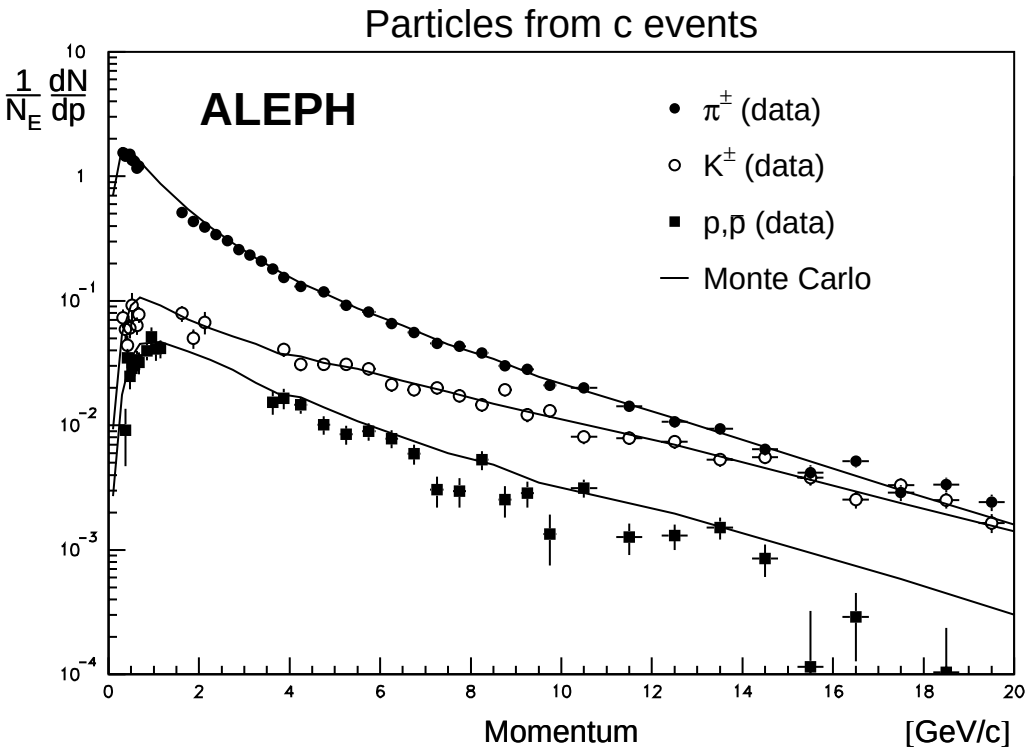

Fig. 8. Momentum spectra from pions, kaons and protons in c events together with the Monte Carlo predictions. The errors shown are the quadratic sum of statistical and systematic errors

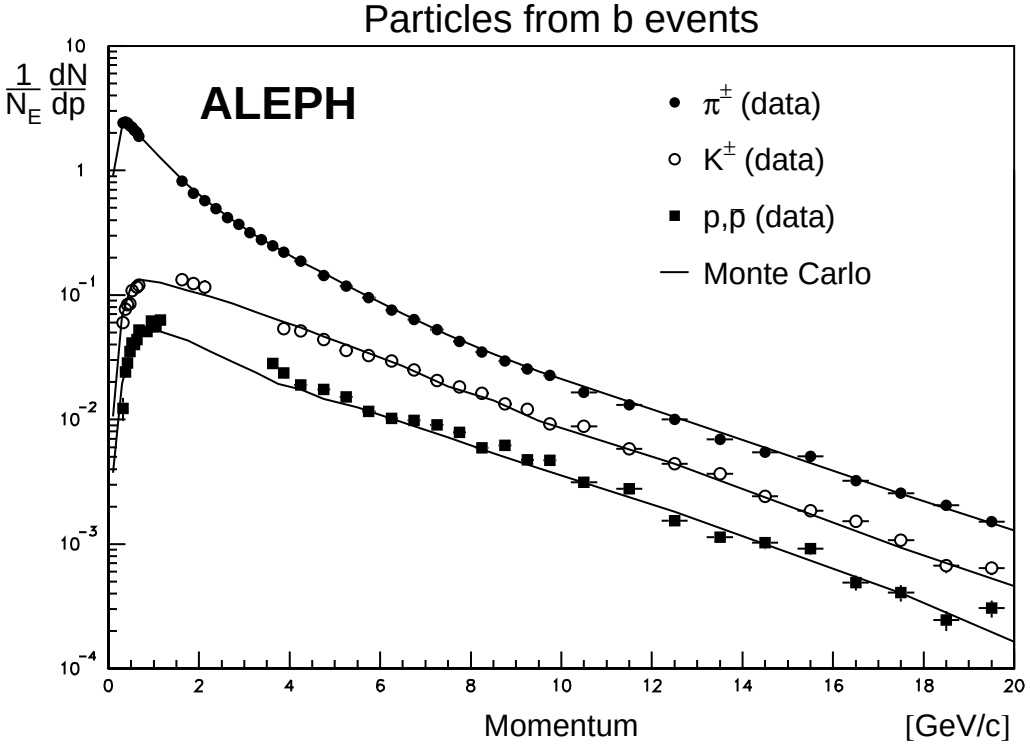

Fig. 9. Momentum spectra from pions, kaons and protons in b events together with the Monte Carlo predictions. The errors shown are the quadratic sum of statistical and systematic errors

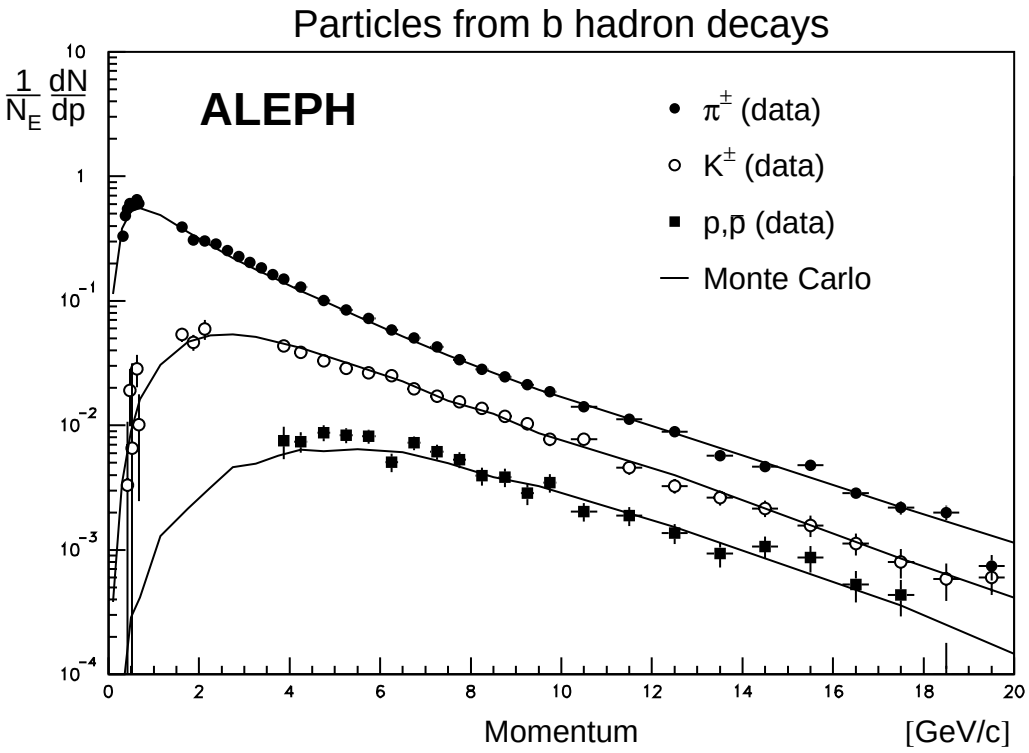

Fig. 10. Momentum spectra from pions, kaons and protons from b-hadron decays together with the Monte Carlo predictions. The errors shown are the quadratic sum of statistical and systematic errors

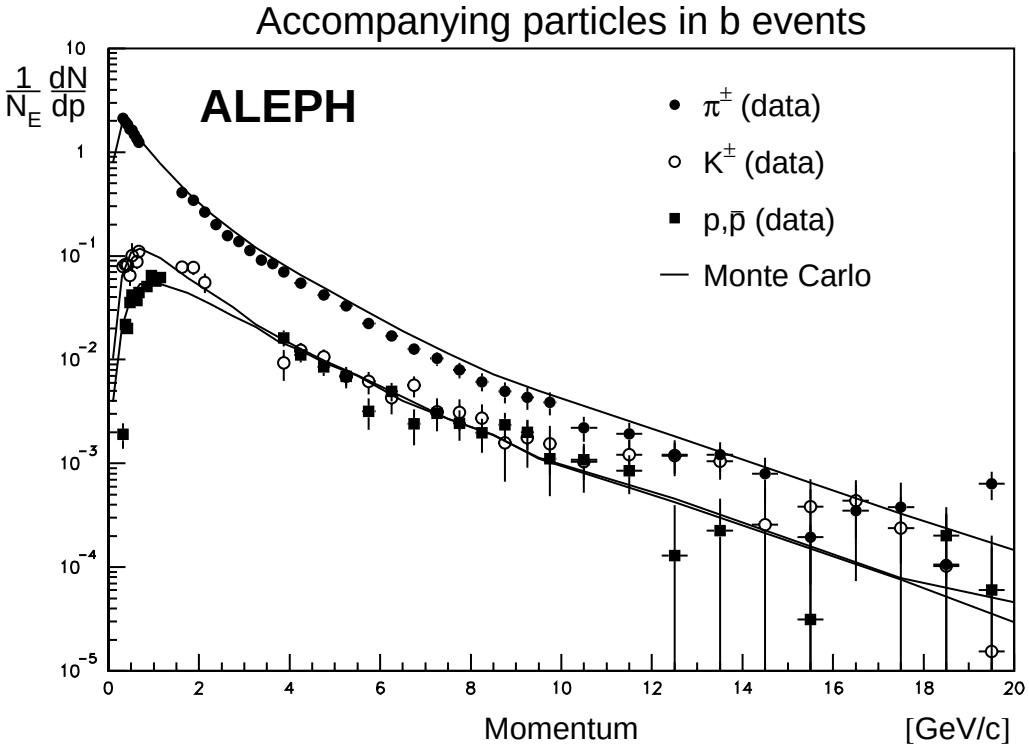

Fig. 11. Momentum spectra of pions, kaons and protons accompanying b-hadrons in b events together with the Monte Carlo predictions. The errors shown are the quadratic sum of statistical and systematic errors

Table 9. The different contributions to the two systematic uncertainties on BR(b-baryon → $pl\bar{\nu}X$). The errors are absolute

Overview of the systematic uncertainties on BR(b-baryon → p$l\bar{\nu}X$)	
1. Systematic uncertainties from the analysis	
dE/dx	0.46%
b-tag	0.34%
Impact parameter	0.23%
p_T spectra	0.19%
lepton selection	0.10%
Extrapolation	0.15%
Reconstr. efficiency	0.11%
Total	0.68%
2. Systematic uncertainties from branching ratios	
BR(b-meson → pX)	0.45%
BR(b-baryon → pX)	0.55%
Total	0.71%

lead to negligible effects. The modelling of the p_T lepton spectra of the background processes is found to be of minor importance compared to that of the spectrum of the signal leptons. The uncertainty was estimated from the divergence between different theoretical predictions for b-meson decay as described in [27]. In addition the rate of four-body semileptonic b-baryon decays has been varied from 0% to 40% and the Λ_b polarization, as measured by ALEPH in [28], was considered. The systematic uncertainties on BR(b-baryon → p$l\bar{\nu}X$) are listed in Table 9.

8 Conclusions

The momentum spectra and mean multiplicities have been measured for pions, kaons and protons in Z → $b\bar{b}$, Z → $c\bar{c}$ and Z → $u\bar{u}, d\bar{d}, s\bar{s}$ separately. In b events, particles from b-hadron decay were distinguished from non-leading particles. The b-baryon fraction and the absolute semileptonic branching ratio BR(b-baryon → p$l\bar{\nu}$X) have been evaluated from proton production and correlated proton-lepton production in b-hadron decays. The b-baryon fraction was estimated from the overall number of protons from b decays and was found to be

$$f_{\Lambda_b} = (10.2 \pm 0.7_{\rm stat} \pm 2.7_{\rm sys})\% \ . \qquad (22)$$

This result was used for the measurement of the absolute branching ratio of the decay b-baryon → p$l\bar{\nu}X$.

$$\text{BR(b-baryon} \to \text{p}l\bar{\nu}X) = (4.63 \pm 0.72_{\rm stat} \pm 0.98_{\rm sys})\% \ . \qquad (23)$$

The ratio R_{pl} =BR(b-baryon → p$l\bar{\nu}X$)/BR(b-baryon → pX) has been found to be

$$R_{pl} = 0.080 \pm 0.012_{\rm stat} \pm 0.014_{\rm sys} \ . \qquad (24)$$

This relatively small number supports the small lifetime of b-baryons with respect to b-mesons as measured at LEP.

Acknowledgements. We wish to thank our colleagues from the accelerator divisions for the successful operation of the LEP machine, and the engineers and technical staff in all our institutions for their contribution to the good performance of ALEPH. Those of us from non-member states thank CERN for its hospitality.

Appendix

Table 10. Pions from uds events normalized to the total nsumber of events N_E. The systematic uncertainties of different momentum bins in the overlap region are correlated

p interval [GeV/c]	$\frac{1}{N_E}\frac{dN}{dp}$	$\Delta_{\rm stat}$	$\Delta_{\rm sys}$
0.30–0.35	6.34 ±	0.04	±0.19
0.35–0.40	6.33 ±	0.04	±0.19
0.40–0.45	5.95 ±	0.03	±0.18
0.45–0.50	5.68 ±	0.03	±0.18
0.50–0.55	5.47 ±	0.03	±0.16
0.55–0.60	5.14 ±	0.02	±0.15
0.60–0.65	4.89 ±	0.02	±0.15
0.65–0.70	4.49 ±	0.02	±0.14
1.50–1.75	1.98 ±	0.01	±0.06
1.75–2.00	1.61 ±	0.01	±0.05
2.00–2.25	1.36 ±	0.01	±0.04
2.25–2.50	1.19 ±	0.01	±0.04
2.50–2.75	1.01 ±	0.01	±0.03
2.75–3.00	0.906 ±	0.004	±0.029
3.00–3.25	0.784 ±	0.003	±0.025
3.25–3.50	0.694 ±	0.003	±0.022
3.50–3.75	0.621 ±	0.003	±0.020
3.75–4.00	0.562 ±	0.003	±0.018
4.00–4.50	0.487 ±	0.002	±0.016
4.50–5.00	0.397 ±	0.002	±0.013
5.00–5.50	0.334 ±	0.002	±0.011
5.50–6.00	0.283 ±	0.002	±0.010
6.00–6.50	0.245 ±	0.001	±0.008
6.50–7.00	0.214 ±	0.001	±0.007
7.00–7.50	0.183 ±	0.001	±0.006
7.50–8.00	0.156 ±	0.001	±0.005
8.00–8.50	0.136 ±	0.001	±0.004
8.50–9.00	0.122 ±	0.001	±0.004
9.00–9.50	0.107 ±	0.001	±0.003
9.50–10.00	0.0975 ±	0.0009	± 0.0031
10.00–11.00	0.0791 ±	0.0006	± 0.0025
11.00–12.00	0.0644 ±	0.0005	± 0.0021
12.00–13.00	0.0516 ±	0.0004	± 0.0017
13.00–14.00	0.0407 ±	0.0004	± 0.0013
14.00–15.00	0.0343 ±	0.0004	± 0.0011
15.00–16.00	0.0283 ±	0.0003	± 0.0009
16.00–17.00	0.0223 ±	0.0003	± 0.0007
17.00–18.00	0.0197 ±	0.0003	± 0.0006
18.00–19.00	0.0150 ±	0.0002	± 0.0005
19.00–20.00	0.0123 ±	0.0002	± 0.0004

Table 11. Kaons from uds events normalized to the total number of events N_E. The systematic uncertainties of different momentum bins in the overlap region are correlated

p interval [GeV/c]	$\frac{1}{N_E} \cdot \frac{dN}{dp}$	$\Delta_{\rm stat}$	$\Delta_{\rm sys}$
.30–.35	$.170 \cdot 10^{+0}$	$\pm .110 \cdot 10^{-1}$	$\pm .594 \cdot 10^{-2}$
.35–.40	$.214 \cdot 10^{+0}$	$\pm .890 \cdot 10^{-2}$	$\pm .749 \cdot 10^{-2}$
.40–.45	$.250 \cdot 10^{+0}$	$\pm .679 \cdot 10^{-2}$	$\pm .874 \cdot 10^{-2}$
.45–.50	$.259 \cdot 10^{+0}$	$\pm .738 \cdot 10^{-2}$	$\pm .905 \cdot 10^{-2}$
.50–.55	$.249 \cdot 10^{+0}$	$\pm .178 \cdot 10^{-1}$	$\pm .871 \cdot 10^{-2}$
.60–.65	$.321 \cdot 10^{+0}$	$\pm .706 \cdot 10^{-2}$	$\pm .112 \cdot 10^{-1}$
.65–.70	$.321 \cdot 10^{+0}$	$\pm .709 \cdot 10^{-2}$	$\pm .112 \cdot 10^{-1}$
1.50–1.75	$.280 \cdot 10^{+0}$	$\pm .461 \cdot 10^{-2}$	$\pm .168 \cdot 10^{-1}$
1.75–2.00	$.256 \cdot 10^{+0}$	$\pm .486 \cdot 10^{-2}$	$\pm .154 \cdot 10^{-1}$
2.00–2.25	$.225 \cdot 10^{+0}$	$\pm .675 \cdot 10^{-2}$	$\pm .135 \cdot 10^{-1}$
3.75–4.00	$.938 \cdot 10^{-1}$	$\pm .270 \cdot 10^{-2}$	$\pm .563 \cdot 10^{-2}$
4.00–4.50	$.899 \cdot 10^{-1}$	$\pm .161 \cdot 10^{-2}$	$\pm .540 \cdot 10^{-2}$
4.50–5.00	$.782 \cdot 10^{-1}$	$\pm .147 \cdot 10^{-2}$	$\pm .469 \cdot 10^{-2}$
5.00–5.50	$.676 \cdot 10^{-1}$	$\pm .140 \cdot 10^{-2}$	$\pm .405 \cdot 10^{-2}$
5.50–6.00	$.592 \cdot 10^{-1}$	$\pm .126 \cdot 10^{-2}$	$\pm .355 \cdot 10^{-2}$
6.00–6.50	$.556 \cdot 10^{-1}$	$\pm .140 \cdot 10^{-2}$	$\pm .334 \cdot 10^{-2}$
6.50–7.00	$.499 \cdot 10^{-1}$	$\pm .110 \cdot 10^{-2}$	$\pm .300 \cdot 10^{-2}$
7.00–7.50	$.443 \cdot 10^{-1}$	$\pm .104 \cdot 10^{-2}$	$\pm .266 \cdot 10^{-2}$
7.50–8.00	$.417 \cdot 10^{-1}$	$\pm .101 \cdot 10^{-2}$	$\pm .250 \cdot 10^{-2}$
8.00–8.50	$.409 \cdot 10^{-1}$	$\pm .957 \cdot 10^{-3}$	$\pm .245 \cdot 10^{-2}$
8.50–9.00	$.336 \cdot 10^{-1}$	$\pm .950 \cdot 10^{-3}$	$\pm .202 \cdot 10^{-2}$
9.00–9.50	$.345 \cdot 10^{-1}$	$\pm .883 \cdot 10^{-3}$	$\pm .207 \cdot 10^{-2}$
9.50–10.00	$.290 \cdot 10^{-1}$	$\pm .806 \cdot 10^{-3}$	$\pm .174 \cdot 10^{-2}$
10.00–11.00	$.291 \cdot 10^{-1}$	$\pm .546 \cdot 10^{-3}$	$\pm .175 \cdot 10^{-2}$
11.00–12.00	$.228 \cdot 10^{-1}$	$\pm .479 \cdot 10^{-3}$	$\pm .137 \cdot 10^{-2}$
12.00–13.00	$.204 \cdot 10^{-1}$	$\pm .443 \cdot 10^{-3}$	$\pm .123 \cdot 10^{-2}$
13.00–14.00	$.177 \cdot 10^{-1}$	$\pm .414 \cdot 10^{-3}$	$\pm .106 \cdot 10^{-2}$
14.00–15.00	$.151 \cdot 10^{-1}$	$\pm .396 \cdot 10^{-3}$	$\pm .907 \cdot 10^{-3}$
15.00–16.00	$.130 \cdot 10^{-1}$	$\pm .352 \cdot 10^{-3}$	$\pm .777 \cdot 10^{-3}$
16.00–17.00	$.112 \cdot 10^{-1}$	$\pm .295 \cdot 10^{-3}$	$\pm .674 \cdot 10^{-3}$
17.00–18.00	$.946 \cdot 10^{-2}$	$\pm .291 \cdot 10^{-3}$	$\pm .568 \cdot 10^{-3}$
18.00–19.00	$.771 \cdot 10^{-2}$	$\pm .268 \cdot 10^{-3}$	$\pm .463 \cdot 10^{-3}$
19.00–20.00	$.704 \cdot 10^{-2}$	$\pm .240 \cdot 10^{-3}$	$\pm .422 \cdot 10^{-3}$

Table 12. Protons from uds events normalized to the total number of events N_E. The systematic uncertainties of different momentum bins in the overlap region are correlated

p interval [GeV/c]	$\frac{1}{N_E}\frac{dN}{dp}$	$\Delta_{\rm stat}$	$\Delta_{\rm sys}$
0.30–0.35	0.0319	± 0.0058	± 0.0010
0.35–0.40	0.0642	± 0.0045	± 0.0019
0.40–0.45	0.0806	± 0.0046	± 0.0024
0.45–0.50	0.102	± 0.004	± 0.003
0.50–0.55	0.110	± 0.004	± 0.003
0.55–0.60	0.131	± 0.004	± 0.004
0.60–0.65	0.127	± 0.004	± 0.004
0.65–0.70	0.148	± 0.004	± 0.004
0.80–0.90	0.149	± 0.003	± 0.004
0.90–1.00	0.150	± 0.006	± 0.004
1.00–1.10	0.159	± 0.006	± 0.005
1.10–1.20	0.158	± 0.004	± 0.005
3.50–3.75	0.0653	± 0.0025	± 0.0052
3.75–4.00	0.0595	± 0.0019	± 0.0048
4.00–4.50	0.0522	± 0.0011	± 0.0042
4.50–5.00	0.0461	± 0.0010	± 0.0037
5.00–5.50	0.0401	± 0.0009	± 0.0032
5.50–6.00	0.0345	± 0.0008	± 0.0028
6.00–6.50	0.0333	± 0.0008	± 0.0027
6.50–7.00	0.0297	± 0.0007	± 0.0024
7.00–7.50	0.0268	± 0.0006	± 0.0021
7.50–8.00	0.0245	± 0.0006	± 0.0020
8.00–8.50	0.0202	± 0.0006	± 0.0016
8.50–9.00	0.0190	± 0.0005	± 0.0015
9.00–9.50	0.0162	± 0.0005	± 0.0013
9.50–10.00	0.0166	± 0.0005	± 0.0013
10.00–11.00	0.0124	± 0.0003	± 0.0010
11.00–12.00	0.0115	± 0.0003	± 0.0009
12.00–13.00	0.00933	±0.00026	± 0.00075
13.00–14.00	0.00746	±0.00026	± 0.00060
14.00–15.00	0.00627	±0.00024	± 0.00050
15.00–16.00	0.00561	±0.00021	± 0.00045
16.00–17.00	0.00454	±0.00017	± 0.00036
17.00–18.00	0.00404	±0.00016	± 0.00032
18.00–19.00	0.00316	±0.00014	± 0.00025
19.00–20.00	0.00287	±0.00013	± 0.00023

Table 13. Pions from c events normalized to the total number of events N_E. The systematic uncertainties of different momentum bins in the overlap region are correlated

p interval [GeV/c]	$\frac{1}{N_E}\frac{dN}{dp}$	$\Delta_{\rm stat}$	$\Delta_{\rm sys}$
0.30–0.35	1.54	± 0.05	± 0.120
0.35–0.40	1.46	± 0.05	± 0.12
0.40–0.45	1.48	± 0.04	± 0.12
0.45–0.50	1.51	± 0.04	± 0.12
0.50–0.55	1.34	± 0.04	± 0.11
0.55–0.60	1.32	± 0.03	± 0.11
0.60–0.65	1.16	± 0.03	± 0.09
0.65–0.70	1.20	± 0.03	± 0.10
1.50–1.75	0.511	± 0.021	± 0.041
1.75–2.00	0.431	± 0.017	± 0.035
2.00–2.25	0.390	± 0.010	± 0.031
2.25–2.50	0.341	± 0.008	± 0.027
2.50–2.75	0.304	± 0.007	± 0.024
2.75–3.00	0.259	± 0.008	± 0.021
3.00–3.25	0.233	± 0.005	± 0.019
3.25–3.50	0.209	± 0.005	± 0.017
3.50–3.75	0.180	± 0.005	± 0.014
3.75–4.00	0.154	± 0.004	± 0.012
4.00–4.50	0.130	± 0.003	± 0.010
4.50–5.00	0.118	± 0.003	± 0.009
5.00–5.50	0.092	± 0.002	± 0.007
5.50–6.00	0.0816	± 0.0021	± 0.0065
6.00–6.50	0.0658	± 0.0019	± 0.0053
6.50–7.00	0.0555	± 0.0018	± 0.0044
7.00–7.50	0.0455	± 0.0016	± 0.0036
7.50–8.00	0.0430	± 0.0015	± 0.0034
8.00–8.50	0.0382	± 0.0014	± 0.0031
8.50–9.00	0.0300	± 0.0013	± 0.0024
9.00–9.50	0.0281	± 0.0012	± 0.0023
9.50–10.00	0.0209	± 0.0011	± 0.0017
10.00–11.00	0.0200	± 0.0007	± 0.0016
11.00–12.00	0.0143	± 0.0006	± 0.0011
12.00–13.00	0.0107	± 0.0005	± 0.0009
13.00–14.00	0.00941	±0.00048	± 0.00075
14.00–15.00	0.00642	±0.00044	± 0.00051
15.00–16.00	0.00419	±0.00045	± 0.00034
16.00–17.00	0.00514	±0.00036	± 0.00041
17.00–18.00	0.00289	±0.00034	± 0.00023
18.00–19.00	0.00336	±0.00034	± 0.00027
19.00–20.00	0.00242	±0.00029	± 0.00019

Table 14. Kaons from c events normalized to the total number of events N_E. The systematic uncertainties of different momentum bins in the overlap region are correlated

p interval [GeV/c]	$\frac{1}{N_E}\frac{dN}{dp}$	$\Delta_{\rm stat}$	$\Delta_{\rm sys}$
0.30–0.35	0.0726	± 0.0103	± 0.0058
0.35–0.40	0.0588	± 0.0085	± 0.0047
0.40–0.45	0.0441	± 0.0070	± 0.0035
0.45–0.50	0.0603	± 0.0084	± 0.0048
0.50–0.55	0.0920	± 0.0223	± 0.0074
0.60–0.65	0.0636	± 0.0081	± 0.0051
0.65–0.70	0.0777	± 0.0083	± 0.0062
1.50–1.75	0.0790	± 0.0057	± 0.0095
1.75–2.00	0.0501	± 0.0061	± 0.0065
2.00–2.25	0.0674	± 0.0085	± 0.0108
3.75–4.00	0.0408	± 0.0032	± 0.0041
4.00–4.50	0.0309	± 0.0020	± 0.0031
4.50–5.00	0.0310	± 0.0018	± 0.0031
5.00–5.50	0.0309	± 0.0016	± 0.0031
5.50–6.00	0.0285	± 0.0015	± 0.0029
6.00–6.50	0.0212	± 0.0015	± 0.0021
6.50–7.00	0.0194	± 0.0013	± 0.0019
7.00–7.50	0.0201	± 0.0012	± 0.0020
7.50–8.00	0.0173	± 0.0011	± 0.0017
8.00–8.50	0.0146	± 0.0011	± 0.0015
8.50–9.00	0.0193	± 0.0011	± 0.0019
9.00–9.50	0.0121	± 0.0009	± 0.0012
9.50–10.00	0.0131	± 0.0009	± 0.0013
10.00–11.00	0.00808	±0.00057	± 0.00081
11.00–12.00	0.00792	±0.00050	± 0.00079
12.00–13.00	0.00736	±0.00044	± 0.00074
13.00–14.00	0.00532	±0.00041	± 0.00053
14.00–15.00	0.00554	±0.00039	± 0.00055
15.00–16.00	0.00381	±0.00036	± 0.00038
16.00–17.00	0.00252	±0.00029	± 0.00025
17.00–18.00	0.00330	±0.00028	± 0.00033
18.00–19.00	0.00251	±0.00027	± 0.00025
19.00–20.00	0.00165	±0.00023	± 0.00017

Table 15. Protons from c events normalized to the total number of events N_E. The systematic uncertainties of different momentum bins in the overlap region are correlated

p interval [GeV/c]	$\frac{1}{N_E}\frac{dN}{dp}$	$\Delta_{\rm stat}$	$\Delta_{\rm sys}$
0.30–0.35	0.00073	± 0.00530	± 0.00062
0.35–0.40	0.0092	± 0.0043	± 0.0007
0.40–0.45	0.0350	± 0.0047	± 0.0028
0.45–0.50	0.0247	± 0.0044	± 0.0020
0.50–0.55	0.0287	± 0.0047	± 0.0023
0.55–0.60	0.0308	± 0.0047	± 0.0025
0.60–0.65	0.0334	± 0.0048	± 0.0027
0.65–0.70	0.0321	± 0.0052	± 0.0026
0.80–0.90	0.0395	± 0.0040	± 0.0032
0.90–1.00	0.0513	± 0.0078	± 0.0041
1.00–1.10	0.0413	± 0.0069	± 0.0033
1.10–1.20	0.0414	± 0.0048	± 0.0033
3.50–3.75	0.0133	± 0.0032	± 0.0015
3.75–4.00	0.0165	± 0.0023	± 0.0018
4.00–4.50	0.0146	± 0.0014	± 0.0016
4.50–5.00	0.0101	± 0.0012	± 0.0011
5.00–5.50	0.00850	± 0.00107	± 0.00094
5.50–6.00	0.00896	± 0.00095	± 0.00099
6.00–6.50	0.00783	± 0.00091	± 0.00086
6.50–7.00	0.00593	± 0.00082	± 0.00065
7.00–7.50	0.00303	± 0.00076	± 0.00033
7.50–8.00	0.00297	± 0.00071	± 0.00033
8.00–8.50	0.00530	± 0.00066	± 0.00058
8.50–9.00	0.00254	± 0.00065	± 0.00028
9.00–9.50	0.00287	± 0.00058	± 0.00032
9.50–10.00	0.00134	± 0.00056	± 0.00015
10.00–11.00	0.00315	± 0.00035	± 0.00035
11.00–12.00	0.00127	± 0.00032	± 0.00014
12.00–13.00	0.00130	± 0.00026	± 0.00014
13.00–14.00	0.00152	± 0.00025	± 0.00017
14.00–15.00	0.000853	±0.000227	± 0.000094
15.00–16.00	0.000116	±0.000208	± 0.000013
16.00–17.00	0.000290	±0.000159	± 0.000032
17.00–18.00	0.000016	±0.000148	± 0.000002
18.00–19.00	0.000000	±0.000131	± 0.000011
19.00–20.00	0.000000	±0.000170	± 0.000019

Table 16. Pions from b events normalized to the total number of events N_E. The systematic uncertainties of different momentum bins in the overlap region are correlated

p interval [GeV/c]	$\frac{1}{N_E}\frac{dN}{dp}$	$\Delta_{\rm stat}$	$\Delta_{\rm sys}$
0.30–0.35	2.41	± 0.02	± 0.07
0.35–0.40	2.46	± 0.02	± 0.08
0.40–0.45	2.42	± 0.02	± 0.08
0.45–0.50	2.29	± 0.01	± 0.07
0.50–0.55	2.22	± 0.01	± 0.07
0.55–0.60	2.09	± 0.01	± 0.06
0.60–0.65	2.03	± 0.01	± 0.06
0.65–0.70	1.87	± 0.01	± 0.06
1.50–1.75	0.817	± 0.008	± 0.029
1.75–2.00	0.657	± 0.007	± 0.024
2.00–2.25	0.573	± 0.004	± 0.021
2.25–2.50	0.492	± 0.003	± 0.018
2.50–2.75	0.415	± 0.003	± 0.015
2.75–3.00	0.372	± 0.003	± 0.013
3.00–3.25	0.317	± 0.002	± 0.011
3.25–3.50	0.277	± 0.002	± 0.010
3.50–3.75	0.248	± 0.002	± 0.009
3.75–4.00	0.220	± 0.002	± 0.008
4.00–4.50	0.186	± 0.001	± 0.007
4.50–5.00	0.144	± 0.001	± 0.005
5.00–5.50	0.118	± 0.001	± 0.004
5.50–6.00	0.0950	± 0.0008	± 0.0034
6.00–6.50	0.0757	± 0.0007	± 0.0027
6.50–7.00	0.0632	± 0.0006	± 0.0023
7.00–7.50	0.0530	± 0.0006	± 0.0019
7.50–8.00	0.0421	± 0.0005	± 0.0015
8.00–8.50	0.0349	± 0.0005	± 0.0013
8.50–9.00	0.0296	± 0.0004	± 0.0011
9.00–9.50	0.0256	± 0.0004	± 0.0009
9.50–10.00	0.0225	± 0.0004	± 0.0008
10.00–11.00	0.0164	± 0.0002	± 0.0006
11.00–12.00	0.0131	± 0.0002	± 0.0005
12.00–13.00	0.0100	± 0.0002	± 0.0004
13.00–14.00	0.00691	±0.00015	± 0.00025
14.00–15.00	0.00547	±0.00014	± 0.00020
15.00–16.00	0.00505	±0.00018	± 0.00018
16.00–17.00	0.00321	±0.00012	± 0.00012
17.00–18.00	0.00255	±0.00013	± 0.00009
18.00–19.00	0.00205	±0.00011	± 0.00007
19.00–20.00	0.00150	±0.00011	± 0.00005

Table 17. Kaons from b events normalized to the total number of events N_E. The systematic uncertainties of different momentum bins in the overlap region are correlated

p interval [GeV/c]	$\frac{1}{N_E}\frac{dN}{dp}$	Δ_{stat}	Δ_{sys}
0.30–0.35	0.0601	± 0.0035	± 0.0024
0.35–0.40	0.0772	± 0.0032	± 0.0031
0.40–0.45	0.0837	± 0.0027	± 0.0034
0.45–0.50	0.0855	± 0.0032	± 0.0034
0.50–0.55	0.108	± 0.008	± 0.004
0.60–0.65	0.116	± 0.003	± 0.005
0.65–0.70	0.120	± 0.003	± 0.005
1.50–1.75	0.133	± 0.002	± 0.009
1.75–2.00	0.123	± 0.002	± 0.011
2.00–2.25	0.115	± 0.003	± 0.016
3.75–4.00	0.0536	± 0.0012	± 0.0032
4.00–4.50	0.0513	± 0.0008	± 0.0031
4.50–5.00	0.0438	± 0.0007	± 0.0026
5.00–5.50	0.0360	± 0.0006	± 0.0022
5.50–6.00	0.0327	± 0.0006	± 0.0020
6.00–6.50	0.0296	± 0.0005	± 0.0018
6.50–7.00	0.0250	± 0.0005	± 0.0015
7.00–7.50	0.0206	± 0.0004	± 0.0012
7.50–8.00	0.0183	± 0.0004	± 0.0011
8.00–8.50	0.0162	± 0.0004	± 0.0010
8.50–9.00	0.0134	± 0.0004	± 0.0008
9.00–9.50	0.0121	± 0.0003	± 0.0007
9.50–10.00	0.00923	± 0.00030	± 0.00055
10.00–11.00	0.00883	± 0.00020	± 0.00053
11.00–12.00	0.00581	± 0.00017	± 0.00035
12.00–13.00	0.00440	± 0.00014	± 0.00026
13.00–14.00	0.00366	± 0.00013	± 0.00022
14.00–15.00	0.00242	± 0.00012	± 0.00015
15.00–16.00	0.00186	± 0.00012	± 0.00011
16.00–17.00	0.00153	± 0.00009	± 0.00009
17.00–18.00	0.00107	± 0.00009	± 0.00006
18.00–19.00	0.000671	±0.000074	± 0.000040
19.00–20.00	0.000639	±0.000065	± 0.000038

Table 18. Protons from b events normalized to the total number of events N_E. The systematic uncertainties of different momentum bins in the overlap region are correlated

p interval [GeV/c]	$\frac{1}{N_E}\frac{dN}{dp}$	Δ_{stat}	Δ_{sys}
0.30–0.35	0.0123	± 0.0024	± 0.0005
0.35–0.40	0.0241	± 0.0017	± 0.0010
0.40–0.45	0.0284	± 0.0016	± 0.0011
0.45–0.50	0.0353	± 0.0017	± 0.0014
0.50–0.55	0.0413	± 0.0018	± 0.0017
0.55–0.60	0.0400	± 0.0017	± 0.0016
0.60–0.65	0.0438	± 0.0018	± 0.0018
0.65–0.70	0.0525	± 0.0020	± 0.0021
0.80–0.90	0.0511	± 0.0015	± 0.0020
0.90–1.00	0.0616	± 0.0030	± 0.0025
1.00–1.10	0.0565	± 0.0029	± 0.0023
1.10–1.20	0.0631	± 0.0018	± 0.0025
3.50–3.75	0.0290	± 0.0013	± 0.0026
3.75–4.00	0.0237	± 0.0009	± 0.0021
4.00–4.50	0.0189	± 0.0005	± 0.0017
4.50–5.00	0.0175	± 0.0005	± 0.0016
5.00–5.50	0.0152	± 0.0004	± 0.0014
5.50–6.00	0.0116	± 0.0004	± 0.0010
6.00–6.50	0.0102	± 0.0003	± 0.0010
6.50–7.00	0.00988	± 0.00031	± 0.00089
7.00–7.50	0.00903	± 0.00029	± 0.00081
7.50–8.00	0.00787	± 0.00027	± 0.00071
8.00–8.50	0.00591	± 0.00024	± 0.00053
8.50–9.00	0.00618	± 0.00024	± 0.00056
9.00–9.50	0.00476	± 0.00022	± 0.00043
9.50–10.00	0.00469	± 0.00021	± 0.00042
10.00–11.00	0.00313	± 0.00013	± 0.00028
11.00–12.00	0.00277	± 0.00012	± 0.00025
12.00–13.00	0.00154	± 0.00009	± 0.00014
13.00–14.00	0.00113	± 0.00007	± 0.00010
14.00–15.00	0.00102	± 0.00007	± 0.00009
15.00–16.00	0.000915	±0.000073	± 0.000082
16.00–17.00	0.000490	±0.000055	± 0.000044
17.00–18.00	0.000406	±0.000053	± 0.000037
18.00–19.00	0.000245	±0.000041	± 0.000022
19.00–20.00	0.000305	±0.000041	± 0.000028

Table 19. Pions from b-hadron decays normalized to the total number of events N_E. The systematic uncertainties of different momentum bins in the overlap region are correlated

p interval [GeV/c]	$\frac{1}{N_E}\frac{dN}{dp}$	$\Delta_{\rm stat}$	$\Delta_{\rm sys}$
0.30–0.35	0.330 ±	0.017	± 0.017
0.35–0.40	0.482 ±	0.014	± 0.024
0.40–0.45	0.548 ±	0.013	± 0.027
0.45–0.50	0.605 ±	0.013	± 0.030
0.50–0.55	0.580 ±	0.012	± 0.029
0.55–0.60	0.601 ±	0.012	± 0.030
0.60–0.65	0.651 ±	0.012	± 0.033
0.65–0.70	0.604 ±	0.012	± 0.030
1.50–1.75	0.393 ±	0.009	± 0.020
1.75–2.00	0.307 ±	0.009	± 0.015
2.00–2.25	0.302 ±	0.006	± 0.015
2.25–2.50	0.285 ±	0.005	± 0.014
2.50–2.75	0.253 ±	0.005	± 0.013
2.75–3.00	0.227 ±	0.004	± 0.011
3.00–3.25	0.202 ±	0.003	± 0.010
3.25–3.50	0.183 ±	0.003	± 0.009
3.50–3.75	0.163 ±	0.003	± 0.008
3.75–4.00	0.149 ±	0.003	± 0.007
4.00–4.50	0.129 ±	0.002	± 0.006
4.50–5.00	0.101 ±	0.002	± 0.005
5.00–5.50	0.0848 ±	0.0016	± 0.0042
5.50–6.00	0.0722 ±	0.0015	± 0.0036
6.00–6.50	0.0583 ±	0.0013	± 0.0029
6.50–7.00	0.0502 ±	0.0012	± 0.0025
7.00–7.50	0.0425 ±	0.0012	± 0.0021
7.50–8.00	0.0336 ±	0.0010	± 0.0017
8.00–8.50	0.0281 ±	0.0010	± 0.0014
8.50–9.00	0.0245 ±	0.0009	± 0.0012
9.00–9.50	0.0212 ±	0.0009	± 0.0011
9.50–10.00	0.0186 ±	0.0008	± 0.0009
10.00–11.00	0.0141 ±	0.0005	± 0.0007
11.00–12.00	0.0112 ±	0.0004	± 0.0006
12.00–13.00	0.00893 ±	0.00039	± 0.00045
13.00–14.00	0.00573 ±	0.00033	± 0.00029
14.00–15.00	0.00466 ±	0.00030	± 0.00023
15.00–16.00	0.00478 ±	0.00033	± 0.00024
16.00–17.00	0.00286 ±	0.00024	± 0.00014
17.00–18.00	0.00219 ±	0.00024	± 0.00011
18.00–19.00	0.00200 ±	0.00025	± 0.00010
19.00–20.00	0.000739 ±	0.000166	± 0.000037

Table 20. Kaons from b-hadron decays normalized to the total number of events N_E. The systematic uncertainties of different momentum bins in the overlap region are correlated

p interval [GeV/c]	$\frac{1}{N_E}\frac{dN}{dp}$	$\Delta_{\rm stat}$	$\Delta_{\rm sys}$
0.30–0.35	−.0174 ±	0.0092	± 0.0009
0.35–0.40	−.00368 ±	0.0085	± 0.00065
0.40–0.45	0.00331 ±	0.00735	± 0.00087
0.45–0.50	0.0191 ±	0.0091	± 0.001
0.50–0.55	0.00656 ±	0.02480	± 0.00033
0.60–0.65	0.0284 ±	0.0078	± 0.0014
0.65–0.70	0.0101 ±	0.0076	± 0.0005
1.50–1.75	0.0536 ±	0.0044	± 0.0054
1.75–2.00	0.0466 ±	0.0045	± 0.0051
2.00–2.25	0.0596 ±	0.0061	± 0.0089
3.75–4.00	0.0436 ±	0.0023	± 0.0035
4.00–4.50	0.0387 ±	0.0014	± 0.0031
4.50–5.00	0.0330 ±	0.0013	± 0.0026
5.00–5.50	0.0288 ±	0.0012	± 0.0023
5.50–6.00	0.0263 ±	0.0011	± 0.0021
6.00–6.50	0.0250 ±	0.0010	± 0.0020
6.50–7.00	0.0196 ±	0.0009	± 0.0016
7.00–7.50	0.0172 ±	0.0009	± 0.0014
7.50–8.00	0.0154 ±	0.0008	± 0.0012
8.00–8.50	0.0137 ±	0.0008	± 0.0011
8.50–9.00	0.0118 ±	0.0007	± 0.0009
9.00–9.50	0.0103 ±	0.0007	± 0.0008
9.50–10.00	0.00774 ±	0.00062	± 0.00062
10.00–11.00	0.00773 ±	0.00041	± 0.00062
11.00–12.00	0.00457 ±	0.00036	± 0.00037
12.00–13.00	0.00326 ±	0.00031	± 0.00026
13.00–14.00	0.00263 ±	0.00028	± 0.00021
14.00–15.00	0.00216 ±	0.00027	± 0.00017
15.00–16.00	0.00157 ±	0.00027	± 0.00013
16.00–17.00	0.00113 ±	0.00021	± 0.00009
17.00–18.00	0.000801 ±	0.000201	± 0.000064
18.00–19.00	0.000584 ±	0.000188	± 0.000047
19.00–20.00	0.000601 ±	0.000157	± 0.000048

Table 21. Protons from b-hadron decays normalized to the total number of events N_E. The systematic uncertainties of different momentum bins in the overlap region are correlated

p interval [GeV/c]	$\frac{1}{N_E}\frac{dN}{dp}$	$\Delta_{\rm stat}$	$\Delta_{\rm sys}$
3.75–4.00	0.00754	± 0.00212	± 0.00060
4.00–4.50	0.00741	± 0.00126	± 0.00059
4.50–5.00	0.00874	± 0.00107	± 0.00070
5.00–5.50	0.00832	± 0.00095	± 0.00067
5.50–6.00	0.00818	± 0.00084	± 0.00066
6.00–6.50	0.00506	± 0.00076	± 0.00041
6.50–7.00	0.00727	± 0.00072	± 0.00058
7.00–7.50	0.00615	± 0.00067	± 0.00049
7.50–8.00	0.00531	± 0.00063	± 0.00043
8.00–8.50	0.00394	± 0.00057	± 0.00032
8.50–9.00	0.00384	± 0.00058	± 0.00031
9.00–9.50	0.00285	± 0.00052	± 0.00023
9.50–10.00	0.00347	± 0.00052	± 0.00028
10.00–11.00	0.00203	± 0.00031	± 0.00016
11.00–12.00	0.00189	± 0.00029	± 0.00015
12.00–13.00	0.00137	± 0.00023	± 0.00011
13.00–14.00	0.000938	± 0.00020	± 0.00008
14.00–15.00	0.00106	± 0.00020	± 0.00009
15.00–16.00	0.000868	±0.000196	± 0.000069
16.00–17.00	0.000528	±0.000145	± 0.000042
17.00–18.00	0.000434	±0.000137	± 0.000035
18.00–19.00	0.000068	±0.000112	± 0.000005
19.00–20.00	0.000113	±0.000081	± 0.000009

Table 22. Accompanying pions in b events normalized to the total number of events N_E. The systematic uncertainties of different momentum bins in the overlap region are correlated

p interval [GeV/c]	$\frac{1}{N_E}\frac{dN}{dp}$	$\Delta_{\rm stat}$	$\Delta_{\rm sys}$
0.30–0.35	2.12	± 0.03	± 0.11
0.35–0.40	1.97	± 0.02	± 0.10
0.40–0.45	1.86	± 0.02	± 0.10
0.45–0.50	1.67	± 0.02	± 0.08
0.50–0.55	1.63	± 0.02	± 0.08
0.55–0.60	1.47	± 0.02	± 0.07
0.60–0.65	1.35	± 0.02	± 0.07
0.65–0.70	1.24	± 0.02	± 0.06
1.50–1.75	0.405	± 0.014	± 0.020
1.75–2.00	0.346	± 0.012	± 0.017
2.00–2.25	0.263	± 0.008	± 0.013
2.25–2.50	0.201	± 0.006	± 0.010
2.50–2.75	0.157	± 0.006	± 0.008
2.75–3.00	0.137	± 0.005	± 0.007
3.00–3.25	0.112	± 0.004	± 0.006
3.25–3.50	0.0913	± 0.0041	± 0.0046
3.50–3.75	0.0841	± 0.0039	± 0.0042
3.75–4.00	0.0701	± 0.0036	± 0.0035
4.00–4.50	0.0550	± 0.0024	± 0.0028
4.50–5.00	0.0420	± 0.0022	± 0.0021
5.00–5.50	0.0330	± 0.0020	± 0.0017
5.50–6.00	0.0223	± 0.0018	± 0.0011
6.00–6.50	0.0169	± 0.0017	± 0.0008
6.50–7.00	0.0127	± 0.0015	± 0.0006
7.00–7.50	0.0102	± 0.0014	± 0.0005
7.50–8.00	0.00796	± 0.00128	± 0.00040
8.00–8.50	0.00613	± 0.00117	± 0.00031
8.50–9.00	0.00493	± 0.00109	± 0.00025
9.00–9.50	0.00434	± 0.00103	± 0.00022
9.50–10.00	0.00387	± 0.00096	± 0.00019
10.00–11.00	0.00222	± 0.00059	± 0.00011
11.00–12.00	0.00192	± 0.00053	± 0.00010
12.00–13.00	0.00121	± 0.00045	± 0.00006
13.00–14.00	0.00122	± 0.00038	± 0.00006
14.00–15.00	0.000793	±0.000342	± 0.000040
15.00–16.00	0.000194	±0.000372	± 0.000010
16.00–17.00	0.000349	±0.000275	± 0.000017
17.00–18.00	0.000381	±0.000271	± 0.000019
18.00–19.00	0.000106	±0.000272	± 0.000005
19.00–20.00	0.000636	±0.000191	± 0.000032

Table 23. Accompanying kaons in b events normalized to the total number of events N_E. The systematic uncertainties of different momentum bins in the overlap region are correlated

p interval [GeV/c]	$\frac{1}{N_E}\frac{dN}{dp}$	$\Delta_{\rm stat}$	$\Delta_{\rm sys}$
0.30–0.35	0.0789	± 0.0113	± 0.0040
0.35–0.40	0.0823	± 0.0103	± 0.0041
0.40–0.45	0.0819	± 0.0087	± 0.0041
0.45–0.50	0.0643	± 0.0107	± 0.0032
0.50–0.55	0.101	± 0.029	± 0.005
0.60–0.65	0.0881	± 0.0094	± 0.0044
0.65–0.70	0.110	± 0.009	± 0.006
1.50–1.75	0.0784	± 0.0055	± 0.0086
1.75–2.00	0.0768	± 0.0057	± 0.0100
2.00–2.25	0.0555	± 0.0077	± 0.0089
3.75–4.00	0.00934	± 0.00291	± 0.00075
4.00–4.50	0.0122	± 0.0018	± 0.0010
4.50–5.00	0.0106	± 0.0016	± 0.0008
5.00–5.50	0.00690	± 0.00144	± 0.00055
5.50–6.00	0.00615	± 0.00134	± 0.00049
6.00–6.50	0.00429	± 0.00124	± 0.00034
6.50–7.00	0.00563	± 0.00114	± 0.00045
7.00–7.50	0.00315	± 0.00106	± 0.00025
7.50–8.00	0.00311	± 0.00099	± 0.00025
8.00–8.50	0.00273	± 0.00093	± 0.00022
8.50–9.00	0.00158	± 0.00090	± 0.00013
9.00–9.50	0.00176	± 0.00083	± 0.00014
9.50–10.00	0.00154	± 0.00074	± 0.00012
10.00–11.00	0.00104	± 0.00050	± 0.00008
11.00–12.00	0.00122	± 0.00043	± 0.00010
12.00–13.00	0.00119	± 0.00037	± 0.00010
13.00–14.00	0.00105	± 0.00034	± 0.00008
14.00–15.00	0.000256	±0.000314	± 0.000020
15.00–16.00	0.000384	±0.000314	± 0.000031
16.00–17.00	0.000438	±0.000245	± 0.000035
17.00–18.00	0.000239	±0.000239	± 0.000019
18.00–19.00	0.000103	±0.000218	± 0.000008
19.00–20.00	0.000015	±0.000187	± 0.000001

Table 24. Accompanying protons in b events normalized to the total number of events N_E. The systematic uncertainties of different momentum bins in the overlap region are correlated

p interval [GeV/c]	$\frac{1}{N_E}\frac{dN}{dp}$	$\Delta_{\rm stat}$	$\Delta_{\rm sys}$
0.30–0.35	0.00190	± 0.00050	± 0.00010
0.35–0.40	0.0218	± 0.0011	± 0.0011
0.40–0.45	0.0200	± 0.0010	± 0.0010
0.45–0.50	0.0357	± 0.0013	± 0.0018
0.50–0.55	0.0421	± 0.0014	± 0.0021
0.55–0.60	0.0396	± 0.0013	± 0.0020
0.60–0.65	0.0371	± 0.0012	± 0.0019
0.65–0.70	0.0444	± 0.0014	± 0.0022
0.80–0.90	0.0509	± 0.0012	± 0.0025
0.90–1.00	0.0645	± 0.0025	± 0.0032
1.00–1.10	0.0574	± 0.0022	± 0.0029
1.10–1.20	0.0621	± 0.0014	± 0.0031
3.50–3.75	0.0206	± 0.0007	± 0.0016
3.75–4.00	0.0162	± 0.0026	± 0.0013
4.00–4.50	0.0112	± 0.0015	± 0.0009
4.50–5.00	0.00849	± 0.00131	± 0.00068
5.00–5.50	0.00690	± 0.00116	± 0.00055
5.50–6.00	0.00316	± 0.00103	± 0.00025
6.00–6.50	0.00495	± 0.00093	± 0.00040
6.50–7.00	0.00241	± 0.00089	± 0.00019
7.00–7.50	0.00303	± 0.00082	± 0.00024
7.50–8.00	0.00244	± 0.00077	± 0.00020
8.00–8.50	0.00198	± 0.00070	± 0.00016
8.50–9.00	0.00236	± 0.00070	± 0.00019
9.00–9.50	0.00200	± 0.00062	± 0.00016
9.50–10.00	0.00111	± 0.00062	± 0.00009
10.00–11.00	0.00108	± 0.00037	± 0.00009
11.00–12.00	0.000855	±0.000344	± 0.000068
12.00–13.00	0.000130	±0.000264	± 0.000010
13.00–14.00	0.000225	±0.000233	± 0.000018
14.00–15.00	0.000042	±0.000231	± 0.000003
15.00–16.00	0.000031	±0.000222	± 0.000003
16.00–17.00	0.000041	±0.000165	± 0.000003
17.00–18.00	0.000035	±0.000153	± 0.000003
18.00–19.00	0.000203	±0.000123	± 0.000016
19.00–20.00	0.000444	±0.000092	± 0.000035

References

1. I.I. Bigi, B. Blok, M. Shifman, A. Vainshtein, CERN–TH 7082/93
2. E. Bagan, P. Ball, V.M. Braun, P. Gosdzinsky, Nucl. Phys. **B 432** (1994) 3; Phys. Lett. **B 342**, (1995) 362; E. Bagan, P. Ball, B. Fiol, P. Gosdzinsky, Phys. Lett. **B 351** (1995) 546
3. for a review see e.g. M. Neubert, CERN–TH/96–55 (1996), to appear in International Journal of Modern Physics A, and references there
4. Particle Data Group, "*Review of Particle Physics*", Phys.Rev. **D 54** (1996) 1
5. OPAL collaboration, "*Measurement of the Semileptonic Branching Fraction of Inclusive b Baryon Decays to Λ*", Z. Phys. **C 74** (1997) 423
6. ALEPH collaboration, "*ALEPH: A Detector for Electron-Positron Annihilations at LEP*", NIM **A 294** (1990) 121
7. ALEPH collaboration, "*Performance of the ALEPH detector at LEP*", NIM **A 360** (1995) 481
8. ALEPH collaboration, "*Inclusive $\pi^{\pm}$, $K^{\pm}$, $(p,\bar{p})$ differential cross-sections at the Z resonance*", Z. Phys. **C 66** (1995) 355
9. ALEPH collaboration, "*Update of Electroweak Parameters from Z Decays*", Z. Phys. **C 60** (1993) 71
10. W.B. Atwood et al., NIM **A 306** (1991) 446
11. H.A. Bethe, Ann. Phys. **5** (1930) 324; F. Bloch, Z. Phys. **81** (1933) 363
12. ALEPH collaboration, "*A precise measurement of $\Gamma_{Z\to b\bar{b}/Z\to hadrons}$*", Phys. Lett. **B 313** (1993) 535
13. J.E. Campagne and R. Zitoun, Z. Phys. **C 42** (1989) 469
14. T. Sjöstrand, Computer Physics Commun. **39** (1986) 347; M. Bengtsson and T. Sjöstrand, Computer Physics Commun. **43** (1987) 367
15. ALEPH collaboration, "*Properties of Hadronic Z Decays and Test of QCD Generators*", Z. Phys. **C 55** (1992) 209
16. http://alephwww.cern.ch/ALPUB/paper/paper_97.html

17. DELPHI collaboration, "*Inclusive Measurements of the $K^{\pm}$ and $p, \bar{p}$ Production in Hadronic Z^0 Decays*", Nucl. Phys. **B 444** (1995) 3
18. OPAL collaboration, "*Measurement of the Production Rates of Charged Hadrons in e^+e^- Annihilation at the Z^0*", Z. Phys. **C 63** (1994) 181
19. DELPHI collaboration, "*Production of Charged Particles, K^0_S, $K^{\pm}$, p and Λ in $Z \to b\bar{b}$ Events and in the Decay of b Hadrons*", Phys. Lett. **B 347** (1995) 447
20. ALEPH collaboration, "*Heavy flavour production and decay with prompt leptons in the ALEPH detector*", Z. Phys. **C 62** (1994) 179
21. ALEPH collaboration, "*Measurement of the b forward-backward asymmetry and mixing using high-$p_\perp$ leptons*", Phys. Lett. **B 384** (1996) 414
22. OPAL collaboration, "*Studies of Charged Particle Multiplicities in b Quark Events*", Z. Phys. **C 61** (1994) 209
23. ALEPH collaboration, "*Heavy quark tagging with leptons in the ALEPH detector*", NIM **A 346** (1994) 461
24. DELPHI collaboration, "*Lifetime and production rate of beauty baryons from Z decays*", Z. Phys. **C 68** (1995) 375
25. ARGUS collaboration, "*Inclusive production of charged pions, kaons and protons in $\Upsilon(4S)$ decays*", Z. Phys. **C 58** (1993) 191
26. CLEO collaboration, "*Measurement of baryon production in B meson decay*", Phys. Rev. **D 45** (1992) 752
27. The LEP experiments, "*Combining Heavy Flavour Electroweak Measurements at LEP* ", CERN–PPE 96/017 (submitted to Nuclear Instruments and Methods)
28. ALEPH collaboration, "*Measurement of the Λ_b polarization in Z decays*", Phys. Lett. **B 365** (1996) 437